AMERICAN SOCIETY FOR MICROBIOLOGY | Journal of Virology

The Interferon-Stimulated Gene IFITM3 Restricts Infection and Pathogenesis of Arthritogenic and Encephalitic Alphaviruses

Subhajit Poddar,[a] Jennifer L. Hyde,[b] Matthew J. Gorman,[a] Michael Farzan,[e] Michael S. Diamond[a,b,c,d]

Departments of Pathology and Immunology,[a] Medicine,[b] and Molecular Microbiology[c] and the Center for Human Immunology and Immunotherapy Programs,[d] Washington University School of Medicine, St. Louis, Missouri, USA; Department of Immunobiology and Microbial Sciences, The Scripps Research Institute, Jupiter, Florida, USA[e]

ABSTRACT

Host cells respond to viral infections by producing type I interferon (IFN), which induces the expression of hundreds of interferon-stimulated genes (ISGs). Although ISGs mediate a protective state against many pathogens, the antiviral functions of the majority of these genes have not been identified. IFITM3 is a small transmembrane ISG that restricts a broad range of viruses, including orthomyxoviruses, flaviviruses, filoviruses, and coronaviruses. Here, we show that alphavirus infection is increased in *Ifitm3*$^{-/-}$ and *Ifitm* locus deletion (*Ifitm-del*) fibroblasts and, reciprocally, reduced in fibroblasts transcomplemented with Ifitm3. Mechanistic studies showed that Ifitm3 did not affect viral binding or entry but inhibited pH-dependent fusion. In a murine model of chikungunya virus arthritis, *Ifitm3*$^{-/-}$ mice sustained greater joint swelling in the ipsilateral ankle at days 3 and 7 postinfection, and this correlated with higher levels of proinflammatory cytokines and viral burden. Flow cytometric analysis suggested that *Ifitm3*$^{-/-}$ macrophages from the spleen were infected at greater levels than observed in wild-type (WT) mice, results that were supported by experiments with *Ifitm3*$^{-/-}$ bone marrow-derived macrophages. *Ifitm3*$^{-/-}$ mice also were more susceptible than WT mice to lethal alphavirus infection with Venezuelan equine encephalitis virus, and this was associated with greater viral burden in multiple organs. Collectively, our data define an antiviral role for Ifitm3 in restricting infection of multiple alphaviruses.

IMPORTANCE

The interferon-induced transmembrane protein 3 (IFITM3) inhibits infection of multiple families of viruses in cell culture. Compared to other viruses, much less is known about the antiviral effect of IFITM3 on alphaviruses. In this study, we characterized the antiviral activity of mouse Ifitm3 against arthritogenic and encephalitic alphaviruses using cells and animals with a targeted gene deletion of *Ifitm3* as well as deficient cells transcomplemented with Ifitm3. Based on extensive virological analysis, we demonstrate greater levels of alphavirus infection and disease pathogenesis when Ifitm3 expression is absent. Our data establish an inhibitory role for Ifitm3 in controlling infection of alphaviruses.

The type I interferon (IFN) response is a critical factor that orchestrates innate protection against viral pathogens. Upon detection of pathogen-associated molecular patterns (PAMPs), host cells produce type I IFN, which in turn induces expression of hundreds of IFN-stimulated genes (ISGs). ISGs can inhibit multiple steps of the viral life cycle (e.g., entry, protein translation, assembly, or egress) or modulate the immune response, such as by enhancing the recruitment of leukocytes or promoting B and T cell maturation (1).

IFN-induced transmembrane (IFITM) proteins 1, 2, and 3 were among the first IFN-stimulated genes (ISGs) to be identified (2) and initially were studied for their roles in germ cell homing and maturation. IFITM proteins are approximately 130 amino acids in length and are conserved in most vertebrate species (3). IFITMs have no catalytic subunit but share similar domain architectures consisting of a short N-terminal domain, two antiparallel domains, a conserved intracellular loop, and a hydrophobic C-terminal domain (4, 5). The topology of IFITM3 has been clarified by electron paramagnetic and nuclear magnetic resonance analyses; the N-terminal domain is located inside the cell, whereas the antiparallel domains reside as intramembrane α-helices, followed by the transmembrane C-terminal domain (6). Although IFITM1, -2, and -3 all have reported antiviral activity, IFITM3 exhibits the greatest protection against the broadest range of viruses, including influenza A virus (IAV), flaviviruses (dengue, West Nile [WNV], and Japanese encephalitis viruses), hepaciviruses (hepatitis C virus), filoviruses (Ebola and Marburg viruses), bunyaviruses (Rift Valley fever and La Crosse viruses), rhabdoviruses (vesicular stomatitis virus), coronaviruses (severe acute respiratory syndrome coronavirus [SARS-CoV]), paramyxoviruses (respiratory syncytial virus [RSV]), and reoviruses (7–17). Despite a wealth of *in vitro* data, the antiviral effects of IFITM3 *in vivo* are less well characterized. To date, only IAV and RSV have been shown to have enhanced pathogenesis in Ifitm3-deficient (*Ifitm3*$^{-/-}$) mice (11, 18, 19). In humans, the allelic polymorphism rs12252-C, which results in a splice variant of IFITM3 lacking the first 21 amino-terminal amino acids, correlates with increased morbidity and

Received 6 April 2016 **Accepted** 17 July 2016

Accepted manuscript posted online 20 July 2016

Citation Poddar S, Hyde JL, Gorman MJ, Farzan M, Diamond MS. 2016. The interferon-stimulated gene IFITM3 restricts infection and pathogenesis of arthritogenic and encephalitic alphaviruses. J Virol 90:8780–8794. doi:10.1128/JVI.00655-16.

Editor: A. García-Sastre, Icahn School of Medicine at Mount Sinai

Address correspondence to Michael S. Diamond, diamond@borcim.wustl.edu.

mortality following IAV infection (19–21). However, some studies have questioned the significance of this truncated IFITM3 allele in the susceptibility to IAV and other viral infections (22, 23).

The mechanisms by which IFITM3 restricts viral infection are not fully elucidated. Studies have shown that IFITM3 affects pH-dependent fusion in the late endosome, which potentially traps entering virions in a hemifusion state (24–26). IFITM3 expression also can modulate the efficiency of cathepsin-mediated proteolysis in an as-yet-undefined manner, which is required for the cleavage of the fusion proteins of reoviruses, filoviruses, and coronaviruses and release of the viral genome from the endolysosome into the cytosol (9, 15). Additionally, IFITM3 is incorporated into the plasma membrane of budding HIV particles, which restricts their fusogenic capability (27). Finally, ectopic expression of IFITMs appears to alter the physical characteristics of the endosome, resulting in increased size, reduced membrane fluidity, and increased cholesterol content, which subsequently impact the efficiency of viral fusion (26, 28, 29).

Alphaviruses are enveloped single-stranded positive-sense RNA viruses of the *Togaviridae* family, many of which are transmitted by mosquitoes. The binding, entry, and pH-dependent fusion of alphaviruses are directed by the structural glycoproteins E1 and E2 (30, 31). E1 and E2 are arranged as heterodimers and assembled into trimeric spikes on the surface of the virion (32). E1 is classified as a type II membrane fusion protein, whereas E2 contains the putative receptor binding site (30).

Chikungunya virus (CHIKV) has emerged rapidly over the last decade, causing outbreaks in the islands of the Indian Ocean, in southern Europe, and in Southeast Asia. In 2013, CHIKV spread to the Western Hemisphere and by the end of 2015 had infected more than 1.7 million people in North, Central, and South America (33). Other arthritogenic alphaviruses have a more limited distribution in parts of Oceania, Africa, and South America, whereas outbreaks of encephalitic alphaviruses occur sporadically in North, Central, and South America (34). Infection by arthritogenic alphaviruses, including CHIKV and Sindbis (SINV), Ross River, and Mayaro viruses, results in a febrile illness associated with rash, myalgia, and moderate to severe joint pain (35). The musculoskeletal disease caused by these viruses is associated with direct infection of myocytes, synovial fibroblasts, and osteoblasts (35–39) and the ensuing infiltration of inflammatory cells. Infection by encephalitic alphaviruses, including Venezuelan (VEEV), Eastern, and Western equine encephalitis viruses, causes a severe febrile illness associated with infection and injury to neurons, encephalitis, long-term debilitating neurological sequelae, and death (34). To date, there are no licensed alphavirus vaccines available for use in humans.

Several ISGs have been characterized as restriction factors against alphavirus infection, including *ISG15*, *PKR*, *ZAP*, and *BST-2*; these genes target viral protein translation and virion egress, respectively (40–44). Ectopic expression-based screens against alphaviruses also have revealed putative inhibitory genes, including *Isg20*, *Ifit1*, *Ifit2*, *Ifit3*, and *Rsad2* (45). However, in the case of *Ifit1*, which recognizes RNA lacking a 2′-O methylation on the 5′ cap structure and prevents translation, alphaviruses subvert its antiviral function via RNA secondary structure motifs that inhibit binding (46). Recent studies suggest that ectopic expression of IFITM genes in cell culture can restrict infection of Sindbis (SINV) and Semliki Forest (SFV) viruses in cell culture by inhibiting viral fusion with cellular membranes (47). Other ISGs (e.g., *HSPE* and *P2RY6*) have been identified, with little information regarding their mechanism of restriction (48, 49). Finally, ISGs can act in synergy to inhibit alphavirus infection (50).

In this study, we evaluated the antiviral activity of IFITM3 against several alphaviruses by comparing infection of IFN-treated wild-type (WT), *Ifitm3*$^{-/-}$, and *Ifitm* locus deletion (*Ifitm-del*) mouse fibroblasts with CHIKV, SFV, SINV, O'nyong-nyong virus (ONNV), and VEEV. In the absence of *Ifitm3* gene expression, we observed an increase in alphavirus replication *in vitro*, which was inhibited following transcomplementation with Ifitm3. *In vivo*, *Ifitm3*$^{-/-}$ mice inoculated with CHIKV sustained higher viral burdens in the spleen, serum, and joint tissues at early times after infection. This was associated with higher levels of proinflammatory cytokines and increased joint swelling along with greater replication in macrophages in some tissues. Consistent with the latter observation, bone marrow-derived macrophages from *Ifitm3*$^{-/-}$ mice sustained higher levels of CHIKV infection than WT cells. Analogous to our observed phenotypes with CHIKV *in vivo*, *Ifitm3*$^{-/-}$ mice infected with VEEV exhibited greater weight loss and mortality and supported greater replication in the liver, spleen, spinal cord, and brain. Collectively, our data suggest that *Ifitm3* contributes to an early host defense response against multiple alphaviruses of global concern.

MATERIALS AND METHODS

Ethics statement. This study was carried out in accordance with the recommendations in the *Guide for the Care and Use of Laboratory Animals* of the National Institutes of Health (51). The protocols were approved by the Institutional Animal Care and Use Committee at the Washington University School of Medicine (assurance number A3381-01). Dissections and injections were performed under anesthesia that was induced with ketamine hydrochloride and xylazine.

Mice. WT C57BL/6 mice were obtained commercially from Jackson Laboratories. *Ifitm-del* and *Ifitm3*$^{-/-}$ mice have been described previously (52). *Ifitm2*$^{-/-}$ mice were described in reference 73. All transgenic mice were backcrossed to 99% purity using speed congenic analysis (53). Four-week-old mice were inoculated in the left footpad with 10^3 focus-forming units (FFU) of CHIKV-LR in 10 μl of phosphate-buffered saline (PBS). Ankles were measured (width by height) for joint swelling on days 3 and 7 postinfection. On selected days after infection, mice were sacrificed for the collection of serum and tissues. After intracardiac perfusion with PBS, organs were harvested, weighed, and homogenized to determine viral titers by a focus-forming assay. For studies with VEEV, a vaccine-derived recombinant strain with a point mutation (TC83-A3G) was used; this mutation confers partial virulence in WT mice as it restores the capacity to antagonize the inhibitory actions of the ISG *Ifit1* (46). Four-week-old mice were inoculated in the left footpad with 10^6 FFU of VEEV-TC83-A3G in 10 μl of PBS. Mice were followed daily for survival and weighed every 2 days. On selected days, infected mice were sacrificed and organs were harvested as described above.

Flow cytometric analysis of CHIKV-infected splenocytes. Spleens of CHIKV-infected mice were harvested after perfusion with PBS. Splenocytes were obtained by generating a single cell suspension, passaging it through a 70-μm filter, and lysing red blood cells with ACK buffer (Invitrogen). Splenocytes were maintained on ice in PBS supplemented with 2% fetal bovine serum (FBS) and 1 mM EDTA. After blockade of Fcγ receptors with anti-CD16/32 (eBioscience; clone 93), staining for viability (eBioscience; FVD eFluor 506) and cell surface antigens CD45, CD3, CD19, CD3, Ly6G, Ly6C, CD11b, CD11c, major histocompatibility complex (MHC) class II, and F4/80 was performed. Viral antigen (E1 and E2 proteins on the surface of cells) was detected using biotinylated humanized CHK-152 and murine CHK-166 (54), with biotinylated humanized West Nile virus (WNV) E16 and murine WNV E60 (55, 56) serving as

isotype controls, respectively. Secondary staining was followed with streptavidin-conjugated Alexa 647 (Invitrogen). Cells were fixed subsequently using the eBioscience FoxP3 fixation buffer set and processed for flow cytometry with the BD LSRII flow cytometer. Data were analyzed with FlowJo software.

Bio-Plex cytokine assay. To measure cytokine levels, a Bio-Plex Pro assay was performed according to the manufacturer's protocol (Bio-Rad) on homogenized ankle tissues isolated at day 1 and 2 postinfection. The cytokine screen included interleukin-1α (IL-1α), IL-1β, IL-2, IL-3 IL-4, IL-5, IL-6, IL-9, IL-10, IL-12p40, IL-12p70, IL-13, IL-17, eotaxin, granulocyte colony-stimulating factor (G-CSF), granulocyte-macrophage CSF (GM-CSF), gamma interferon (IFN-γ), KC, monocyte chemoattractant protein 1 (MCP-1), macrophage inflammatory protein 1α (MIP-1α), MIP-1β, RANTES (CCL5), and tumor necrosis factor alpha (TNF-α).

Cells and viruses. Primary WT, *Ifitm-del*, *Ifitm2*$^{-/-}$, and *Ifitm3*$^{-/-}$ mouse-derived mouse embryonic fibroblasts (MEFs) and bone marrow-derived macrophages were generated according to published methods (57). Transformed MEFs were generated by transfection of the SV2 plasmid, which encodes the large T antigen of SV2 polyomavirus (58), and passaged ~10 times. All MEFs were cultured in complete Dulbecco's modified Eagle's medium (DMEM), which was supplemented with 10% fetal bovine serum and 10 mM (each) GlutaMAX, sodium pyruvate, nonessential amino acids, and HEPES, pH 7.3. MEFs that ectopically express c-Myc-tagged firefly luciferase or c-Myc-tagged Ifitm3 were generated via lentiviral transduction of the pFCIV vector, which contains an internal ribosome entry site-green fluorescent protein (IRES-GFP) (59, 60). Lentivirus was produced by transfecting 293T cells with pSPAX.2 (Addgene catalog no. 12260), pMD2G (Addgene catalog no. 12259), and pFCIV. Supernatants were harvested at 48 to 72 h posttransfection. WT, *Ifitm-del*, and *Ifitm3*$^{-/-}$ transformed MEFs were incubated with lentiviral supernatants and 10 μg/ml of Polybrene and spinoculated (300 × *g*) at room temperature for 30 min. The inoculum was replaced with complete DMEM 24 h later and incubated at 37°C. Transduction efficiency was determined by expression of GFP, and sorting of GFP^{+} cells was performed on a FACS Aria II cell sorter (Becton, Dickinson). After repeated passages to ensure stable expression, the MEFs were tested for GFP and protein expression by flow cytometry and Western blotting, respectively. Vero and 293T cells were cultured and passaged in complete DMEM.

The CHIKV-LR (La Reunion OPY1 p142) strain was a gift from S. Higgs (Kansas State University). SINV (Toto) was a gift from C. Rice and P. MacDonald (Rockefeller University). VEEV-TC83 was a gift from W. Klimstra (University of Pittsburgh). These strains were produced from infectious cDNA clones (61, 62). CHIKV 181/25, ONNV (MP30), and SFV (Kumba) were provided by the World Reference Center for Arboviruses (R. Tesh, University of Texas Medical Branch). Virus propagation and titration were performed in Vero cells.

Genotyping of MEFs. Genomic DNA was extracted from MEFs with the Qiagen DNeasy blood and tissue kit and was characterized by PCR. The *Ifitm2* WT allele or the knockout (KO) construct was genotyped using the following primers: *Ifitm2* WT F, 5′-ATGTGGTCTGGTCCCTGTTC-3′, and *Ifitm2* WT R, 5′-AGGTGCTCTGGCTCCATTTC-3′ (WT band, 520 bp); *Ifitm2* KO F, 5′-TCATTCTCAGTATTGTTTTGCC-3′, and *Ifitm2* KO R, 5′-TGGAGACCAGAAGCCTGAC-3′ (KO band, 373 bp). PCR conditions for both *Ifitm2* WT and KO alleles were as follows: 94°C for 3 min, 94°C for 45 s, 55°C for 30 s, and 70°C for 1 min 30 s, for 35 cycles, and 70°C for 10 min. The *Ifitm3*$^{-/-}$ mouse can be identified by the in-frame insertion of GFP within the *Ifitm3* allele (52). The WT allele or the knockout construct was genotyped using the following primers: WT *Ifitm3* F, 5′-ATCCTTTGCCCTTCAGTGCT-3′, and WT *Ifitm3* R, 5′-ACTCATACCTCGGTGCCATC-3′ (WT band, 355 bp; KO band, 1,321 bp). PCR conditions for both *Ifitm3* WT and KO were as follows: 94°C for 1 min 30 s, 94°C for 25 s, and 60°C for 30 s, reducing temperature by 0.1°C per cycle; 72°C for 1 min 30 s, 35 cycles; and 72°C for 5 min. The IFITM-del allele was determined using the following primers (52): IFITM-del WT F, 5′-AACATGCCTTGCATCCCTGGAGTTCCTTCTAAAGGA-3′, and IFITM-del WT R, 5′-CCCTAAAACACTTAGCAGTGACCCCTCACAAGCC-3′ (WT band, 500 bp); *Ifitm*-del KO F, 5′-ACTCTAGCCAGAGTCTTGCATTTCTCAGTCCTAAAC-3′, and IFITM-del KO R, 5′-TCTAGTACAGTCGGTAAGAACAAAATAGTGTCTATCA-3′ (KO band, 600 bp). PCR conditions for *Ifitm-del* alleles were as follows: 95°C for 30 s, 54°C for 30 s, and 68°C for 1 min 30 s, for 29 cycles, and 68°C for 5 min.

qRT-PCR measurement of *Ifitm* genes. WT, *Ifitm2*$^{-/-}$, *Ifitm3*$^{-/-}$, and *Ifitm-del* MEFs (10^4 cells per condition) were seeded in a 96-well plate. After 6 h of incubation with IFN-β at various doses, MEFs were lysed and total RNA was extracted with the Qiagen RNeasy kit. *Ifitm2* and *Ifitm3* were detected using quantitative reverse transcription-PCR (qRT-PCR) and normalized to *Gapdh* expression, using the following PrimeTime assays (IDT) according to the manufacturer's instructions: *Ifitm2*, Mm.PT.58.33172327.g; *Ifitm3*, Mm.PT.51.6979575.g; and *Gapdh*, Mm.PT.39a.a.

Western blotting. MEFs were lysed in radioimmunoprecipitation assay (RIPA) buffer and electrophoresed under reducing conditions on a 12% Bis-Tris NuPAGE gel with morpholineethanesulfonic acid (MES) buffer according to the manufacturer's instructions (Thermo Fisher). After transfer onto polyvinylidene difluoride (PVDF) membranes (Thermo Fisher) using an iBlot apparatus (Thermo Fisher), proteins of interest were detected with mouse anti-β-actin (CST; 8H10D10), mouse anti-c-Myc (Sigma; 9E10), goat anti-Ifitm3 (R & D; AF337), horseradish peroxidase (HRP)-conjugated anti-mouse IgG (Sigma Chemical), and HRP-conjugated anti-goat IgG (Santa Cruz; sc2304). For quantification of protein, secondary donkey anti-mouse IRDye 680 (Li-Cor; 925-68072) and anti-rabbit-IRDye 800CW (Li-Cor; 926-32214) were used instead of HRP conjugates and visualized on the Odyssey Imager (Li-Cor). Polyclonal rabbit anti-Ifitm3 (Proteintech; 11714-1-AP) was used for Ifitm3 detection in these experiments. Quantification was performed with Li-Cor Odyssey software.

Virus infection of cells. MEFs were plated (10^4 cells per well) in a 96-well plate and in some experiments pretreated for 6 h with recombinant mouse IFN-β (PBL Assay Science) at concentrations from 5 to 0.1 IU/ml, as indicated in the figure legends. The cells were inoculated with a given alphavirus (multiplicity of infection [MOI] of 5) and incubated at 37°C. At selected time points, cells were trypsinized, fixed with 1% paraformaldehyde (PFA), and permeabilized with Hanks' balanced salt solution (HBSS) containing 0.1% saponin and 10 mM HEPES. Infection was determined after sequentially staining cells with mouse or human monoclonal antibodies (MAbs) (CHIKV, CHK-11; SFV, 2B4; TC83, 1A4A-1; ONNV, 4J21) (54, 63) against the E2 glycoprotein. SINV infection was detected using murine anti-SINV ascites (ATCC; VR-1248AF). Alexa 647-conjugated goat anti-mouse or human IgG antibody (Life Technologies) was used for secondary antibody staining. Samples were processed by flow cytometry using a BD FACSArray cytometer. Data were analyzed with FlowJo software.

For viral yield assays, cells were plated (10^5 cells per well in a 12-well plate) and in some experiments pretreated with specified doses of IFN-β for 12 h. Cells then were infected with CHIKV at 37°C. One hour later, the plates were rinsed twice with warm PBS and replaced with fresh DMEM supplemented with 10% FBS. Supernatants were collected at specific time points, and viral titers were determined by focus-forming assay on Vero cells, as described previously (46, 54). After fixation, infected cell foci were detected with CHK-11 and HRP-conjugated anti-mouse IgG (Sigma Chemical) and quantified with an ImmunoSpot analyzer (Cellular Technologies, Ltd.).

Binding and internalization assays. MEFs were plated (10^5 cells/well in a 24-well plate)on the night before use. Cells were chilled on ice for 10 min, exposed to CHIKV-LR at an MOI of 5, and incubated on ice for 1 h. Unbound virus was removed with repeated washes of chilled medium or PBS. To determine binding efficiency of virus, MEFs were lysed with RNeasy lysis buffer (Qiagen), and RNA was extracted using the RNeasy minikit (Qiagen) and analyzed for CHIKV RNA by qRT-PCR. To determine the efficiency of virus internalization, warm complete DMEM was

added to MEFs and incubated at 37°C for 1 h. Medium was removed, and cells were placed on ice. Proteinase K (500 μg/ml) in ice-cold PBS was added for 1 h to digest any surface-bound virus (64). MEFs were then transferred to Eppendorf tubes and washed with PBS before lysing with RNeasy lysis buffer and extraction of RNA for qRT-PCR. Primer probe sets ordered from IDT were CHIKV (F, 5′-TCGACGCGCCCTCTTTAA-3′; R, 5′-ATCGAATGCACCGCACACT-3′; probe, 5′-/56-FAM [6-carboxyfluorescein]/ACCAGCCTGCACCCATTCCTCAGAC/36-TAMSp/-3′) and the glyceraldehyde-3-phosphate dehydrogenase (*Gapdh*) PrimeTime assay Mm.PT.39a.a.

Fusion-from-without (FFWO) assay. MEFs were rinsed and then incubated with DMEM, supplemented with 0.2% FBS, 10 mM HEPES (pH 7.3), and 20 mM NH_4Cl, on ice for 15 min. Virus (MOI of 100) was added to MEFs on ice for 1 h to allow binding. Unbound virus was removed after several rinses with chilled medium. Subsequently, prewarmed acidic (DMEM, 0.2% FBS, 10 mM HEPES, 30 mM succinic acid, pH 5.5) or neutral (DMEM, 0.2% FBS, 10 mM HEPES, pH 7.4) medium was added for 2 min at 37°C. Medium then was removed and replaced with warmed DMEM-10% FBS-10 mM HEPES supplemented with 20 mM NH_4Cl to inhibit endosomal viral fusion and *de novo* infection via the endosomal pathway. At 6 h after infection, MEFs were fixed with PFA, permeabilized, and analyzed for viral antigen by flow cytometry, as described above.

Statistical analysis. All data were analyzed using Prism software (GraphPad, San Diego, CA). Viral infection assays in cell culture were analyzed by one-way analysis of variance (ANOVA) with Dunnett's multiple-comparison test or Student's *t* test. Viral kinetics assays were analyzed by two-way ANOVA with Dunnett's or Sidak's multiple comparisons. Viral burden assays were analyzed by the Mann-Whitney test. qRT-PCR assays were analyzed by Student's *t* test. Kaplan-Meier survival curves were analyzed by the log rank test.

RESULTS

Restriction of alphaviruses by Ifitm proteins in cell culture. Although expression of IFITM genes inhibits infection of several different genera of viruses (7–16), their antiviral activities against alphaviruses have yet to be established. To test whether Ifitm genes restrict alphavirus infection, we developed MEF lines lacking Ifitm2 (*Ifitm2*$^{-/-}$), Ifitm3 (*Ifitm3*$^{-/-}$), and Ifitm1, -2, -3, -5, and -6 (*Ifitm-del*) (Fig. 1A). To assess their effects on CHIKV replication, MEFs were first pretreated with 1 IU/ml of recombinant mouse IFN-β to induce *Ifitm* gene expression (Fig. 1B). Ifitm3 protein induction was confirmed by Western blotting in WT and *Ifitm2*$^{-/-}$ MEFs after IFN-β treatment, whereas, as expected, *Ifitm3*$^{-/-}$ and *Ifitm-del* MEFs lacked Ifitm3 protein (Fig. 1C). IFN-pretreated MEFs were then infected with a high viral dose (MOI of 5) of pathogenic (CHIKV-La Reunion 2006 [LR]) or attenuated (CHIKV 181/25) strains of CHIKV. Fourteen hours later, cells were harvested, and viral antigen was analyzed by flow cytometry. Whereas *Ifitm3*$^{-/-}$ and *Ifitm-del* MEFs supported greater CHIKV infection (3-fold, $P < 0.01$, and 4-fold, $P < 0.001$, for CHIKV 181/25, respectively; 4.5-fold, $P < 0.0001$, and 6.5-fold, $P < 0.0001$, for CHIKV-LR, respectively) than did WT cells, no increase in viral antigen expression was observed in *Ifitm2*$^{-/-}$ MEFs (Fig. 1D to F). Correspondingly, IFN-β-pretreated *Ifitm3*$^{-/-}$ and *Ifitm-del* MEFs infected with CHIKV produced higher titers of infectious virus than did WT or *Ifitm2*$^{-/-}$ cells (Fig. 1G, CHIKV 181/25, 28-fold for *Ifitm3*$^{-/-}$ [$P < 0.01$] and 12-fold for *Ifitm-del* [$P < 0.05$]; Fig. 1H, CHIKV-LR, 147-fold for *Ifitm3*$^{-/-}$ [$P < 0.0001$] and 36-fold for *Ifitm-del* [$P < 0.0001$]) at 14 h postinfection. These data suggest that Ifitm3 has a dominant antiviral effect on CHIKV infection compared to Ifitm2.

We next tested whether Ifitm3 exhibited antiviral activity against other alphaviruses. Analogous to experiments with CHIKV, WT and Ifitm-deficient MEFs were pretreated with various doses of IFN-β, infected at a high MOI, and assayed by flow cytometry. Notably, *Ifitm3*$^{-/-}$ and *Ifitm-del* MEFs pretreated with IFN-β supported enhanced infection by SFV, ONNV, VEEV (strain TC-83), and SINV compared to WT cells ($P < 0.05$, Fig. 2).

To corroborate our findings, we transcomplemented WT, *Ifitm3*$^{-/-}$, and *Ifitm-del* MEFs with c-Myc-tagged to the N terminus of Ifitm3 or firefly luciferase protein as a control. After confirmation of ectopic protein expression by flow cytometry and Western blotting (Fig. 3A and B), MEFs were infected with CHIKV 181/25 (MOI of 5) in the absence of IFN-β treatment and analyzed at 6 h postinfection. MEFs transcomplemented with Ifitm3 showed less CHIKV replication than firefly luciferase-expressing controls (Fig. 3C and D). These data suggest that Ifitm3 inhibits multiple alphaviruses *in vitro* and does not require expression of Ifitm1, Ifitm2, Ifitm5, and Ifitm6 proteins to exert its antiviral activity.

Ifitm3 inhibits pH-dependent fusion of alphaviruses. Studies with IAV have shown that IFITM3 prevents fusion of virions from the late endosome, which is required for release of viral genomic material into the cytosol (24, 25). Correspondingly, IFITM3 is expressed preferentially on membranes of intracellular vesicles, including endosomes (9). However, following gene upregulation, such as after IFN induction or ectopic expression, IFITM3 can accumulate on the plasma membrane (18, 65, 66), which independently could restrict attachment of viruses to the cell surface. To define the stage in the alphavirus life cycle that Ifitm3 inhibits, we assessed its effect on binding, internalization, and fusion.

To determine if expression of Ifitm3 alters binding of alphaviruses to the cell surface, transcomplemented MEFs were incubated with CHIKV at 4°C for 1 h, washed extensively to remove unbound virus, and assayed by qRT-PCR. As no differences in levels of bound CHIKV genomic RNA were detected between Ifitm3-expressing MEFs and their corresponding controls (Fig. 4A), we concluded that binding efficiency was not appreciably affected. To assess whether Ifitm3 affected internalization, CHIKV was prebound to transcomplemented MEFs for 1 h on ice, followed by incubation at 37°C for 1 h. MEFs then were treated with proteinase K to remove residual surface-bound virus before recovery of cellular RNA. Similarly to cell surface binding assays, we observed no difference in the levels of internalized viral RNA (Fig. 4B). As anticipated, in control binding experiments performed at 4°C, proteinase K treatment significantly decreased (11-fold, $P < 0.0001$) the level of cell-bound viral RNA (Fig. 4C).

As we did not observe effects of Ifitm3 on attachment or internalization, we next evaluated pH-dependent fusion. Alphaviruses can be induced to fuse at the plasma membrane in the presence of an acidic solution (acid bypass or fusion from without [FFWO]) (67), albeit at low efficiency; this required us to infect at a high multiplicity of infection. To test whether FFWO is affected by ectopic expression of Ifitm3, MEFs were preincubated with CHIKV at 4°C, washed to remove unbound virus, and then incubated with prewarmed medium at pH 7.4 or pH 5.5. Subsequently, medium was replaced with normal-pH culture medium supplemented with 20 mM NH_4Cl, which prevents alphavirus maturation and fusion (67) and was added to inhibit productive infection of progeny virions. Fourteen hours later, MEFs were analyzed for viral antigen by flow cytometry. Ifitm3-transcomplemented MEFs had lower levels of CHIKV antigen than luciferase-expressing controls in WT, *Ifitm3*$^{-/-}$, and *Ifitm-*

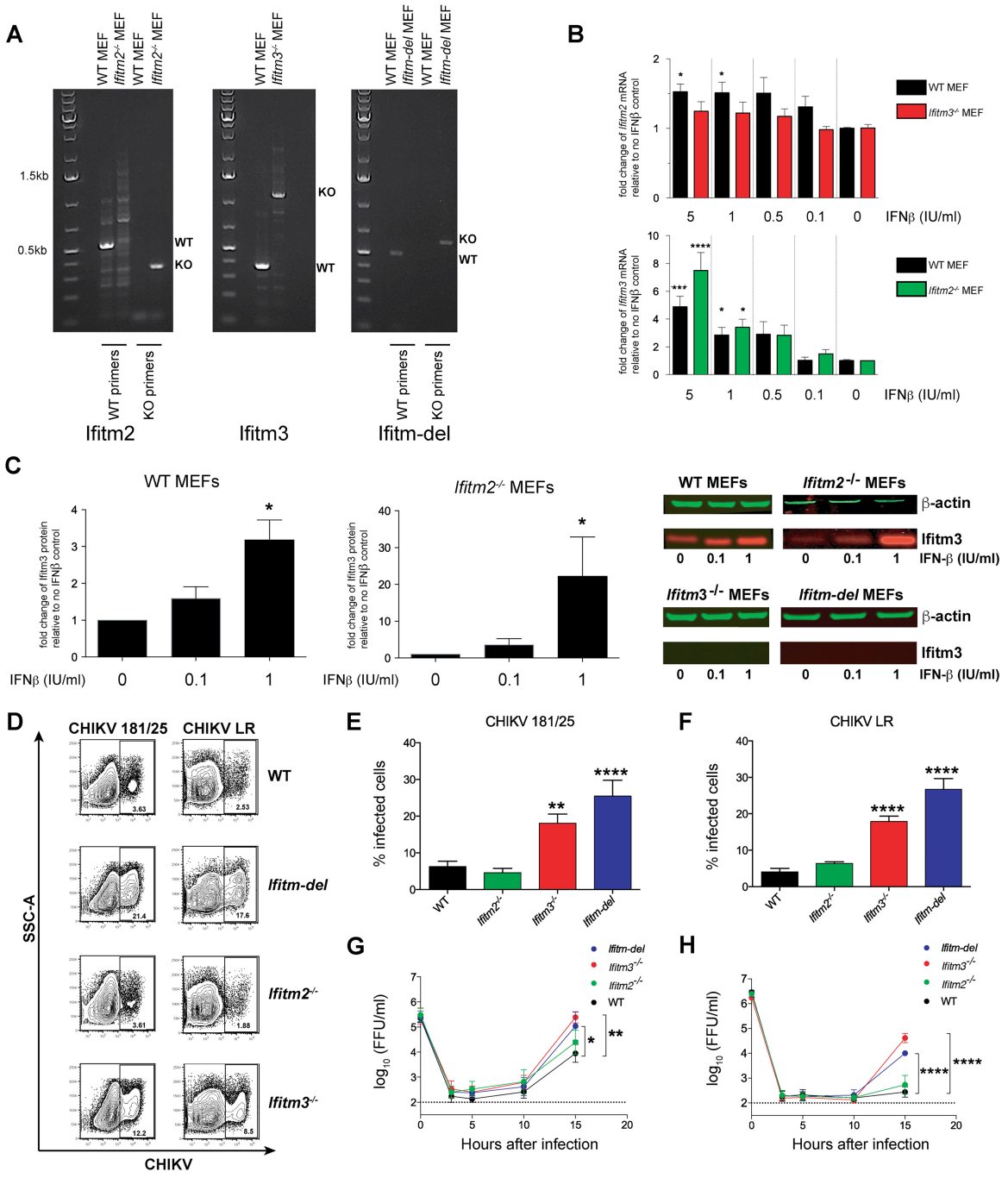

FIG 1 CHIKV infection is enhanced in cells lacking Ifitm3 expression. WT, *Ifitm2*$^{-/-}$, *Ifitm3*$^{-/-}$, and *Ifitm-del* MEFs were generated from WT and gene-targeted mice. (A) Genotyping of MEFs was performed by PCR and agarose electrophoresis. Bands corresponding to WT and KO alleles are indicated to the right of each gel. (B) MEFs were pretreated with various doses of IFN-β and tested for *Ifitm2* and *Ifitm3* gene induction by qRT-PCR. *Ifitm2* expression was not detected in *Ifitm2*$^{-/-}$ and *Ifitm-del* MEFs, and *Ifitm3* expression was not detected in *Ifitm3*$^{-/-}$ and *Ifitm-del* MEFs. Bars show the means and standard errors of the means from three independent experiments performed in duplicate. Means were compared between control and IFN-β-treated cells using a nonparametric one-way ANOVA with Dunn's multiple comparisons (*, $P < 0.05$; ***, $P < 0.001$; ****, $P < 0.0001$). (C) MEFs were pretreated with the indicated doses of IFN-β and tested for Ifitm3 expression by quantitative Western blotting. (Left) Means from three independent experiments were compared between control and IFN-β-treated cells using a nonparametric one-way ANOVA with Dunn's multiple comparisons (*, $P < 0.05$). (Right) A representative Western blot with loading controls (β-actin) is shown. (D to H) The indicated MEFs were pretreated with 1 U/ml of IFN-β and subsequently infected with CHIKV 181/25 or CHIKV-LR at an MOI of 5. (D) At 14 h postinfection, MEFs were stained for viral E2 protein and analyzed by flow cytometry. (E and F) Cumulative flow cytometry data for CHIKV 181/25 and CHIKV-LR. Bars show the means and standard errors of the means (SEM) from five independent experiments performed in quadruplicate or duplicate. Means were compared between WT and deficient cell lines using one-way ANOVA with Dunnett's multiple comparisons (*, $P < 0.05$; **, $P < 0.01$; ***, $P < 0.001$; ****, $P < 0.0001$). (G and H) Kinetics of CHIKV 181/25 and CHIKV-LR replication in IFN-β-pretreated WT, *Ifitm3*$^{-/-}$, and *Ifitm-del* MEFs infected at an MOI of 5. Supernatant was harvested at indicated time points, and virus titers were determined. Curves show the means and standard errors of the means from the pooled data of two or three independent experiments performed in triplicate. Means at each time point were compared between WT and knockout cell lines using two-way ANOVA with Dunnett's multiple comparisons (*, $P < 0.05$; **, $P < 0.01$; ***, $P < 0.001$; ****, $P < 0.0001$).

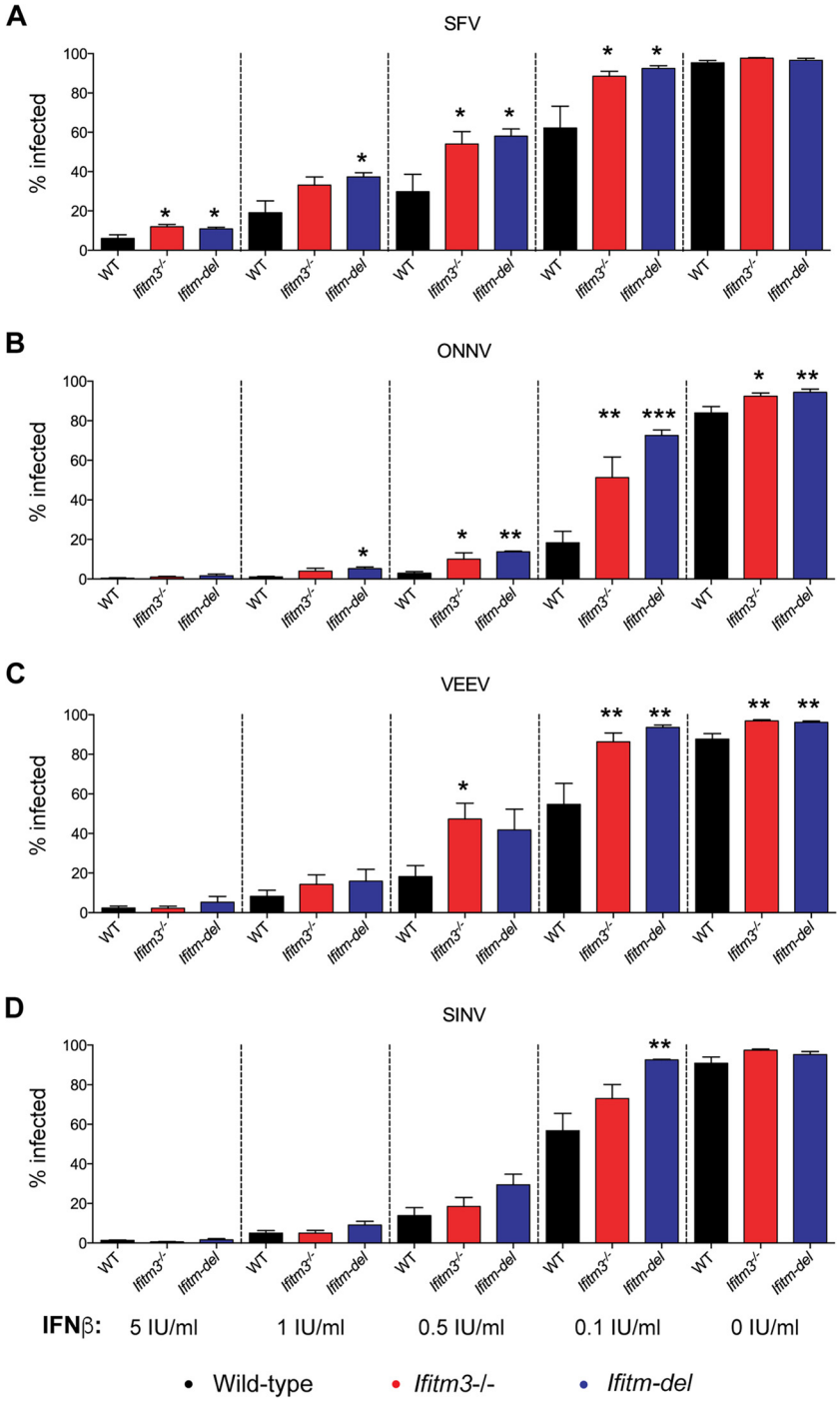

FIG 2 Infection of other alphaviruses is enhanced in cells lacking Ifitm3 expression. WT, *Ifitm3*$^{-/-}$, and *Ifitm-del* MEFs were pretreated with the indicated concentrations of IFN-β and subsequently infected with SFV (A), ONNV (B), VEEV-TC83 (C), or SINV (D) at an MOI of 5. At 14 h postinfection, MEFs were stained for viral E2 proteins and analyzed by flow cytometry. Bars represent the means and standard errors of the means from three independent experiments performed in duplicate. For each concentration of IFN-β, means between WT and knockout cells were compared using one-way ANOVA with Dunnett's multiple comparisons (*, $P < 0.05$; **, $P < 0.01$; ***, $P < 0.001$).

del MEFs (Fig. 4D and E). Consistent with results with IAV (24), expression of Ifitm3 also inhibits pH-dependent fusion of alphaviruses.

Ifitm3 inhibits alphavirus infection *in vivo*. To determine whether Ifitm3 has a protective role against alphaviruses *in vivo*, we used an established mouse model of CHIKV infection and arthritis (68). We inoculated 4-week-old WT and *Ifitm3*$^{-/-}$ mice with CHIKV-LR in the left footpad and measured joint swelling on days 3 and 7 after infection, which correspond to the peaks of tissue edema and cellular infiltrates, respectively (54, 68). Whereas

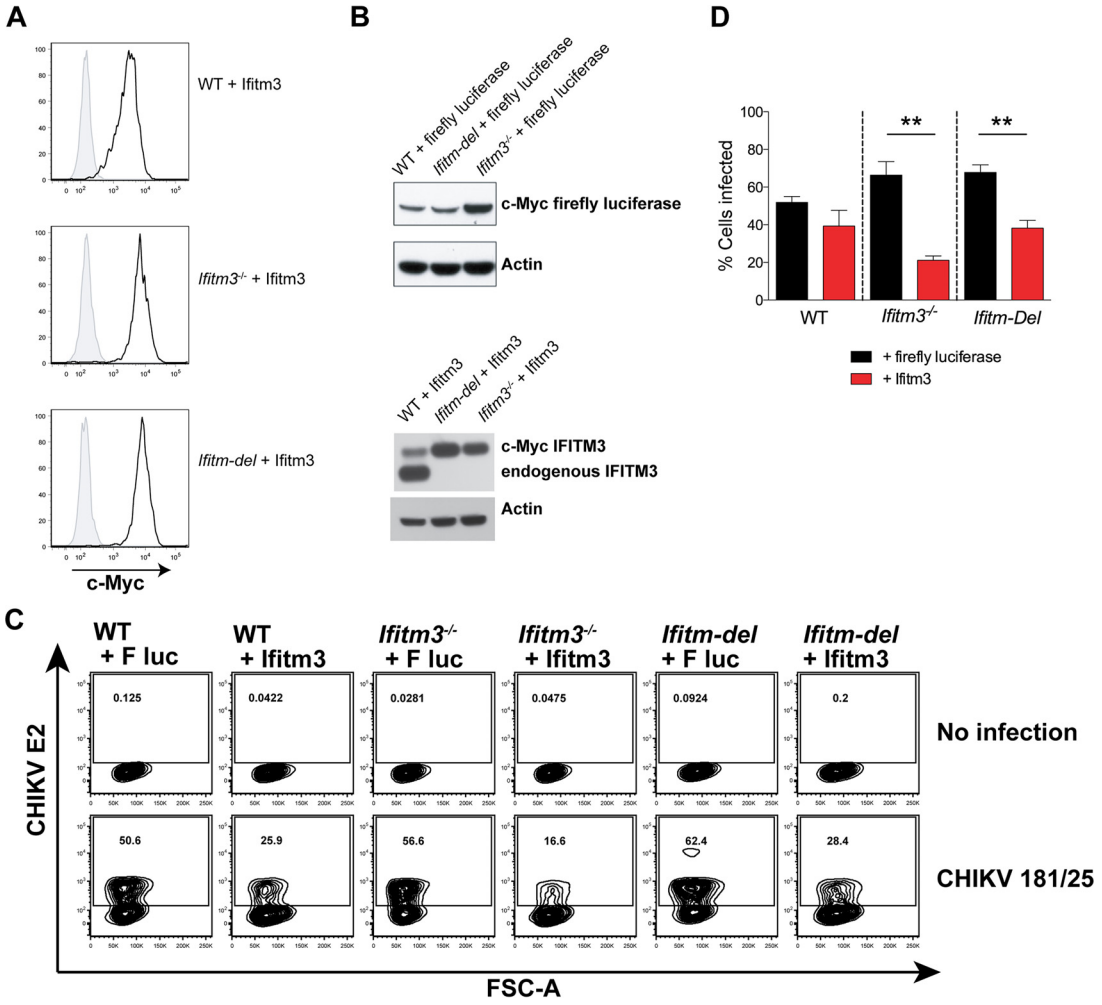

FIG 3 Ectopic expression of IFITM3 inhibits CHIKV infection. c-Myc-tagged firefly luciferase and Ifitm3 were cloned into the pFCIV vector and introduced into WT, *Ifitm3*$^{-/-}$, and *Ifitm-del* MEFs via lentiviral transduction. (A and B) Successful transduction was determined by staining for c-Myc tag by flow cytometry (gray-filled are negative control; black lines, anti-c-Myc) (A) and Western blotting for firefly luciferase (detected with anti-c-Myc antibody) and Ifitm3 (detected with anti-Ifitm3 antibody) in transcomplemented MEFs (B). β-Actin loading controls are provided below each gel. Results are representative of three independent experiments. (C) Flow cytometry contour plots of CHIKV infection in transcomplemented MEFs. Cells were infected for 6 h in the absence of IFN-β with CHIKV 181/25 at an MOI of 5. Infection was determined by flow cytometry of E2-positive cells. (D) Pooled data from CHIKV infection. Bars represent the means and standard errors of the means from three independent experiments done in triplicate. Means were compared by Student's *t* test (**, $P < 0.01$).

no difference was seen in viral titers at these time points (Fig. 5A), greater swelling was observed in ipsilateral ankle joints of *Ifitm3*$^{-/-}$ mice than in WT mice on both days (Fig. 5B and C, $P < 0.001$ and $P < 0.01$, respectively). Because of the disparity between clinical signs and virological data, we analyzed viral burden in different tissues (serum, spleen, ankles, wrists, and quadriceps muscles) at earlier time points (days 1 and 2 after inoculation) (Fig. 5D to K). At day 1 after inoculation, the serum, spleen, and ipsilateral ankle (Fig. 5D to F) of *Ifitm3*$^{-/-}$ mice had higher viral titers than did WT mice (20-fold in serum, $P < 0.0001$; 160-fold in spleen, $P < 0.0001$; and 2.5-fold in ipsilateral ankle, $P < 0.01$). In comparison, at day 2, the titers in the spleen, serum, and ipsilateral ankle were similar but levels in the contralateral ankle and contralateral quadriceps muscle (Fig. 5G and I) were somewhat higher (4.5-fold, $P < 0.001$, and 5-fold $P < 0.01$, respectively). However, by day 3, no differences in viral titer were observed in any tissues between WT and *Ifitm3*$^{-/-}$ mice.

The early higher viral burden in *Ifitm3*$^{-/-}$ mice corresponded to higher levels of inflammatory chemokines and cytokines in the ipsilateral ankle (Table 1). The mean concentrations of several chemokines and cytokines (e.g., IL-2, MCP-1, TNF-α, IL-1α, IL-12p40, G-CSF, and GM-CSF, $P < 0.05$) were higher in ankles from CHIKV-infected *Ifitm3*$^{-/-}$ mice than in those from WT mice at days 1 and/or 2 after infection. These data suggest that in the context of CHIKV infection *in vivo*, Ifitm3 contributes to restriction of early viral infection and spread, which impacts cytokine induction and the development of clinical disease.

Given the increase in viral titers in the spleen of *Ifitm3*$^{-/-}$ mice on day 1, we hypothesized that Ifitm3 might affect the cellular tropism of CHIKV. To identify the cell subsets that were more susceptible to CHIKV infection, we performed flow cytometric analysis on spleens of infected WT and *Ifitm3*$^{-/-}$ mice (Fig. 6A to C). Splenocytes were stained for CHIKV envelope (E1 and E2)

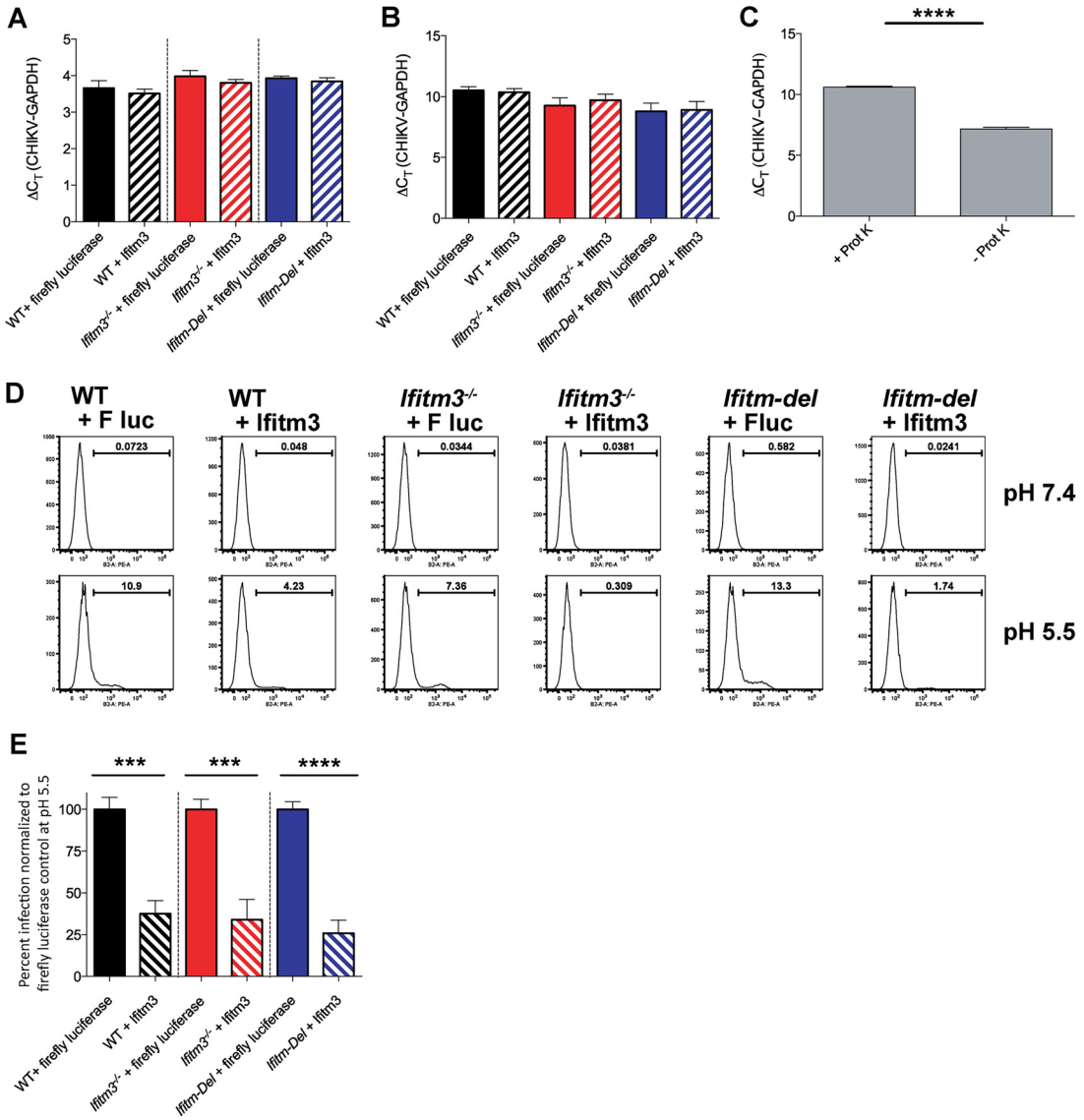

FIG 4 Role of Ifitm3 in restricting CHIKV binding, entry, and pH-dependent fusion. (A) CHIKV-LR was bound to firefly luciferase or Ifitm3-transcomplemented MEFs for 1 h on ice. After repeated rinses with chilled PBS, total RNA was isolated and analyzed for CHIKV RNA by qRT-PCR. Pooled data from 3 independent experiments done in duplicate are shown. (B) After CHIKV-LR binding and washing, MEFs were incubated at 37°C for 1 h to allow for virus internalization. MEFs were then treated with proteinase K on ice for 1 h to digest any bound but not internalized virions, followed by washing, RNA extraction, and analysis by qRT-PCR. Data are representative of three independent experiments performed in duplicate. (C) As a control, we confirmed the efficiency of proteinase K for removing surface-bound (at 4°C) but not internalized CHIKV. MEFs treated with proteinase K had lower levels of CHIKV RNA as detected by qRT-PCR (higher threshold cycle [C_T] values, $P < 0.0001$). (D and E) FFWO assay of CHIKV 181/25 on transcomplemented MEFs. CHIKV (MOI of 100) was bound to cells on ice for 2 h, followed by treatment with neutral (pH 7.4) or acidic (pH 5.5) medium at 37°C for 2 min to induce fusion. Medium was replaced with neutral culture medium supplemented with NH_4Cl and incubated at 37°C for 14 h before analysis of CHIKV antigen-positive cells by flow cytometry. Data represent the means and standard errors of the means from three independent experiments done in triplicate. Means were compared by Student's *t* test (***, $P < 0.001$; ****, $P < 0.0001$).

proteins using specific MAbs (54) and compared to isotype control MAbs. Inflammatory monocytes ($CD11b^+$ $Ly6G^+$), macrophages ($CD11b^{hi}$ $F4/80^{lo}$), and red pulp macrophages ($CD11b^{lo}$ $F4/80^{hi}$) expressed high levels of viral antigen (50%, 50%, and 25%, respectively), with no difference in the fraction of infected cells from WT and *Ifitm3*$^{-/-}$ cells (Fig. 6B and data not shown). Nonetheless, greater numbers of CHIKV antigen-positive $CD11b^{hi}$ $F4/80^{lo}$ and $CD11b^{lo}$ $F4/80^{hi}$ macrophages were detected in the spleens of *Ifitm3*$^{-/-}$ mice than in WT mice (1.3-fold, $P <$ 0.05; 1.7-fold, $P < 0.05$; and 2.2-fold, $P < 0.05$, respectively) (Fig. 6C). An increased number of *Ifitm3*$^{-/-}$ neutrophils expressed CHIKV antigen (1.6-fold, $P < 0.05$), but the overall number of neutrophils was substantially lower than other myeloid cell populations. No differences in viral antigen-positive inflammatory monocytes were observed between the *Ifitm3*$^{-/-}$ and WT controls, and neither *Ifitm3*$^{-/-}$ nor WT $CD4^+$, $CD8^+$, $CD19^+$, or $NK1.1^+$ cells exhibited detectable viral protein staining (data not shown). To determine if *Ifitm3*$^{-/-}$ macrophages can support

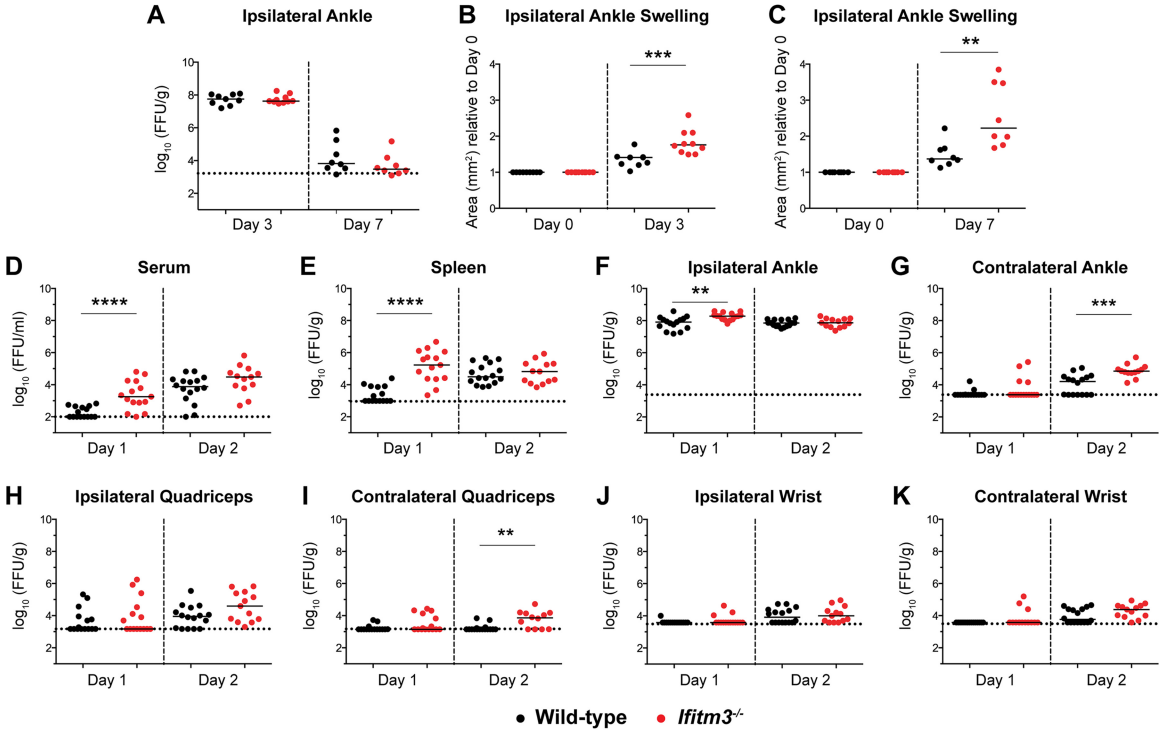

FIG 5 Ifitm3 restricts CHIKV pathogenesis *in vivo*. Four-week-old WT and *Ifitm3*$^{-/-}$ mice were inoculated with 10^3 FFU of CHIKV-LR in the left footpad. (A) Viral titers in the ipsilateral ankle at days 3 and 7 postinfection. Data were pooled from two independent experiments, and each point represents one mouse (n = 8 to 10). The dotted line represents the limit of detection. No statistical difference was seen by the Mann-Whitney test. (B and C) Swelling of the ipsilateral ankle of infected WT and *Ifitm3*$^{-/-}$ mice at days 3 and 7 postinfection. Area was determined by measuring the width and height of the ankle using digital calipers. Data are pooled from two independent experiments and are normalized to the measured area of the ankles just prior to infection. Each dot represents one mouse (n = 8 to 10). Asterisks indicate statistical differences by the Mann-Whitney test (**, $P < 0.01$; ***, $P < 0.001$). (D to K) Four-week-old WT and *Ifitm3*$^{-/-}$ mice were inoculated with 10^3 FFU of CHIKV-LR in the left footpad. Viral burdens in the serum (D), spleen (E), ankles (F and G), muscles (H and I), and wrists (J and K) at days 1 and 2 postinfection were determined by focus-forming assay. Dotted lines represent the limit of detection. Data are pooled from three independent experiments, and each dot represents one mouse (n = 13 to 16). Asterisks indicate statistical differences by the Mann-Whitney test (**, $P < 0.01$; ***, $P < 0.001$; ****, $P < 0.0001$).

greater replication of CHIKV, bone marrow-derived macrophages were cultured from WT and *Ifitm3*$^{-/-}$ mice and infected at an MOI of 0.1. Viral supernatants were collected up to 72 h postinfection and analyzed by focus-forming assay. *Ifitm3*$^{-/-}$ macrophages produced more virus at 24 and 48 h postinfection than did WT cells (Fig. 6D) (12.5-fold, $P < 0.01$, and 10-fold, $P < 0.01$, respectively). These data suggest that a lack of Ifitm3 allows for enhanced CHIKV infection in macrophages.

To assess whether Ifitm3 had a protective effect against other alphaviruses *in vivo*, we infected 4-week-old WT and *Ifitm3*$^{-/-}$ mice with a previously described moderately pathogenic encephalitic alphavirus strain (VEEV-TC83-A3G), which is resistant to the antiviral effects of another ISG, Ifit1 (46). *Ifitm3*$^{-/-}$ mice exhibited greater mortality (Fig. 7A) and morbidity (as judged by weight loss) (Fig. 7B) after VEEV-TC83-A3G infection than did WT mice. Consistent with the clinical phenotypes, higher VEEV titers were observed at day 1 after infection in the liver and spinal cord (3-fold, $P < 0.05$, and 8-fold, $P < 0.01$, respectively) (Fig. 7C) and day 2 after infection in the spleen, brain, and liver of *Ifitm3*$^{-/-}$ mice than in WT mice (2.5-fold, $P < 0.05$; 250-fold, $P < 0.05$; and 10-fold, $P < 0.01$, respectively) (Fig. 7C). These data confirm that Ifitm3 restricts alphavirus infection *in vivo* and prevents early dissemination.

DISCUSSION

To evaluate the potential antiviral role of Ifitm3 in restricting alphaviruses *in vitro*, we infected WT, *Ifitm3*$^{-/-}$, and *Ifitm-del* MEFs with CHIKV, SFV, ONNV, VEEV, and SINV. All alphaviruses tested exhibited some degree of enhanced infection in *Ifitm3*$^{-/-}$ cells. In contrast, studies with CHIKV and *Ifitm2*$^{-/-}$ MEFs showed infection comparable to that of WT MEFs, suggesting that Ifitm2 is not the predominant Ifitm gene responsible for inhibiting alphaviruses in the context of an intact type I IFN response. The antiviral function of Ifitm3 against alphaviruses was validated using transcomplemented MEFs that ectopically express Ifitm3. Analogous to how IFITM3 inhibits IAV infection (24, 26), our mechanism-of-action studies suggest that Ifitm3 does not affect the binding or internalization of CHIKV but instead prevents pH-dependent fusion events.

We also observed greater CHIKV infection and disease pathogenesis *in vivo* in animals lacking Ifitm3 expression. *Ifitm3*$^{-/-}$ mice developed greater ankle swelling than did WT animals, and this difference correlated with an increased viral burden and inflammatory chemokine and cytokine levels at early times postinoculation. Notably, at later time points, titers became equivalent in WT and *Ifitm3*$^{-/-}$ mice, suggesting possible immune evasion of Ifitm3 by CHIKV, which could occur by several previously iden-

TABLE 1 Cytokine levels in joint tissue homogenates after CHIKV infection[a]

		Day 1		Day 2	
Cytokine	Genotype	Mean pg/ml (SEM)	*P*	Mean pg/ml (SEM)	*P*
IL-1α	WT	7.6 (±1.0)	0.2	9.8 (±0.6)	0.03
	Ifitm3$^{-/-}$	12 (±2.4)		14 (±1.5)	
IL-1β	WT	52 (±11)	0.3	144 (±18)	0.2
	Ifitm3$^{-/-}$	71 (±14)		181 (±9.2)	
IL-2	WT	11 (±1.9)	0.03	15 (±1.9)	0.09
	Ifitm3$^{-/-}$	16 (±1.8)		21 (±3.1)	
IL-3	WT	0.33 (±0.06)	0.9	0.39 (±0.08)	0.006
	Ifitm3$^{-/-}$	0.33 (±0.06)		0.76 (±0.06)	
IL-4	WT	3.2 (±0.2)	0.3	4.2 (±0.5)	0.1
	Ifitm3$^{-/-}$	3.2 (±0.5)		6.1 (±1.0)	
IL-5	WT	0.6 (±0.2)	0.9	3.0 (±1.0)	0.7
	Ifitm3$^{-/-}$	0.8 (±0.4)		3.4 (±1.0)	
IL-6	WT	1.5 (±0.4)	0.8	8.8 (±1.1)	0.4
	Ifitm3$^{-/-}$	1.9 (±1.0)		11 (±1.9)	
IL-9	WT	22 (±7.1)	0.9	31 (±9.1)	0.006
	Ifitm3$^{-/-}$	28 (±16)		107 (±24)	
IL-10	WT	1.1 (±0.06)	0.3	3.1 (±0.9)	0.02
	Ifitm3$^{-/-}$	1.3 (±0.2)		5.3 (±0.8)	
IL-12p40	WT	1.1 (±0.2)	0.8	10 (±1.6)	0.02
	Ifitm3$^{-/-}$	1.4 (±0.3)		15 (±0.8)	
IL-12p70	WT	2.8 (±0.2)	0.1	6.2 (±0.7)	0.5
	Ifitm3$^{-/-}$	3.8 (±0.5)		7.0 (±0.6)	
IL-13	WT	LOD (38.7)	0.9	LOD (38.7)	0.9
	Ifitm3$^{-/-}$	44 (±5.7)		39 (±0.8)	
IL-17	WT	0.3 (±0.09)	0.9	0.3 (±0.08)	0.8
	Ifitm3$^{-/-}$	0.3 (±0.1)		0.2 (±0.06)	
Eotaxin	WT	151 (±3.8)	0.5	176 (±11)	0.9
	Ifitm3$^{-/-}$	162 (±8.2)		176 (±12)	
G-CSF	WT	0.7 (±0.1)	0.9	4.2 (±1.2)	0.007
	Ifitm3$^{-/-}$	0.9 (±0.3)		8.5 (±0.8)	
GM-CSF	WT	43 (±4.9)	0.14	59 (±6.4)	0.04
	Ifitm3$^{-/-}$	55 (±5.0)		77 (±5.7)	
IFN-γ	WT	LOD (1.2)	>0.9	1.8 (±0.3)	0.7
	Ifitm3$^{-/-}$	LOD (1.2)		1.5 (±0.14)	
KC	WT	16 (±2.6)	0.6	81 (±15)	0.8
	Ifitm3$^{-/-}$	23 (±5.6)		83 (±13)	
MCP-1	WT	52 (±15)	0.01	706 (±119)	0.4
	Ifitm3$^{-/-}$	118.5 (±25.44)		833 (±70)	
MIP-1α	WT	38 (±1.4)	0.3	168 (±29)	0.8
	Ifitm3$^{-/-}$	50 (±7.8)		151 (±13)	
MIP-1β	WT	20 (±3.9)	0.3	150 (±33)	0.2
	Ifitm3$^{-/-}$	34 (±8.5)		89 (±23)	
RANTES	WT	13 (±2.4)	0.8	109 (±28)	0.8
	Ifitm3$^{-/-}$	12 (±3.1)		88 (±24)	
TNF-α	WT	17 (±3.0)	0.004	48 (±7.5)	0.5
	Ifitm3$^{-/-}$	41 (±6.4)		56 (±7.4)	

[a] Mice were infected with 10^3 FFU of CHIKV-LR in the footpad. Ipsilateral joint tissues were collected at 1 and 2 days after infection, homogenates were prepared, and the indicated cytokines were measured by Bio-Plex array. Data represent the means (±standard errors of the means) in picograms per milliliter from 9 to 11 mice per group. Statistical significance was determined by the Mann-Whitney test. LOD, limit of detection.

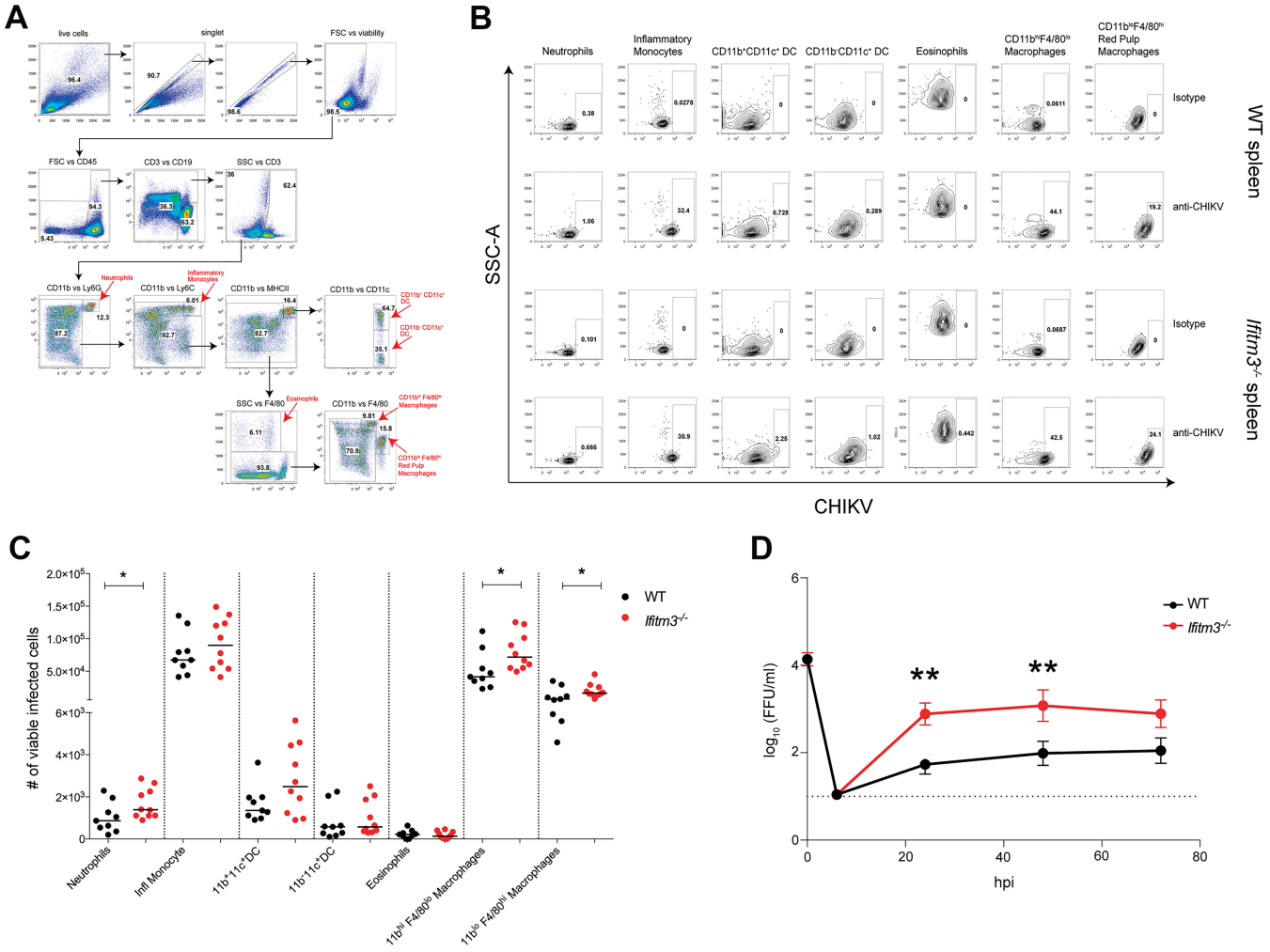

FIG 6 Infection of splenocyte subsets by CHIKV-LR in WT and *Ifitm3*$^{-/-}$ mice. Splenocytes from 4-week-old WT and *Ifitm3*$^{-/-}$ mice were harvested 1 day after infection (10^3 FFU in the footpad); stained for neutrophils, inflammatory monocytes, dendritic cells, eosinophils, macrophages, and red pulp macrophages and for surface expression of CHIKV E1 and E2 viral antigen; and analyzed by flow cytometry. (A) Detailed gating strategy for different cell subsets is shown. FSC, forward scatter; SSC, side scatter. (B) Representative contour plots of WT and *Ifitm3*$^{-/-}$ splenocytes gated for CHIKV antigen-positive cells, stained with either isotype control or anti-CHIKV envelope protein antibody. (C) Scatter plots indicate the number of CHIKV antigen-positive cells for each subpopulation. Data were pooled from two independent experiments. Each dot represents one mouse ($n = 9$ to 10). Asterisks determine statistical differences by the Mann-Whitney test (*, $P < 0.05$). Note the break in the *y* axis. (D) Viral kinetics of CHIKV-LR infection in bone marrow-derived WT and *Ifitm3*$^{-/-}$ macrophages infected at an MOI of 0.1. Data are pooled from five independent experiments performed in triplicate, and each point indicates mean and standard error of the mean. The dotted line indicates the limit of detection. Asterisks determine statistical differences by two-way ANOVA and Sidak's multiple comparisons (**, $P < 0.01$). hpi, hours postinfection.

tified mechanisms, including host transcriptional shutoff (69) or antagonism of IFN signaling (70). To assess possible effects of Ifitm3 on cellular tropism, we assessed CHIKV antigen staining using flow cytometric analysis of splenocytes at day 1 postinfection. These cells were chosen because they were easily profiled and exhibited a substantial (160-fold) difference in viral yield at this time point. Although the overall percentages of CHIKV-positive myeloid cells were similar in the spleens of *Ifitm3*$^{-/-}$ and WT mice, a higher number of macrophages were positive for CHIKV antigen, suggesting a possible role for Ifitm3 in controlling viral growth in these cell types. One limitation of the flow cytometry experiments is that we cannot be certain that CHIKV antigen-positive staining defines bona fide infection, as it remains possible that we are detecting bound/opsonized virus on the surface of cells rather than E1 and E2 proteins prior to budding. To address this issue, we tried infection studies in WT and *Ifitm3*$^{-/-}$ mice with double subgenomic reporter gene viruses (e.g., CHIKV-GFP); however, the fluorescence staining was too dim for conclusive results, possibly because of the attenuation of these viruses. Nonetheless, our studies with bone marrow-derived macrophages support a role for Ifitm3 restriction of CHIKV infection in this cell type, as increased titers were observed in cells from *Ifitm3*$^{-/-}$ mice.

Our *in vivo* findings were not limited to CHIKV, as we also observed greater mortality, weight loss, and viral burden following VEEV infection of *Ifitm3*$^{-/-}$ mice. These data suggest an important role for Ifitm3 in restricting alphavirus pathogenesis *in vivo*, by limiting replication and dissemination early during infection. Future studies using analogous flow cytometric approaches and conditional gene deletions are planned to define the cell-

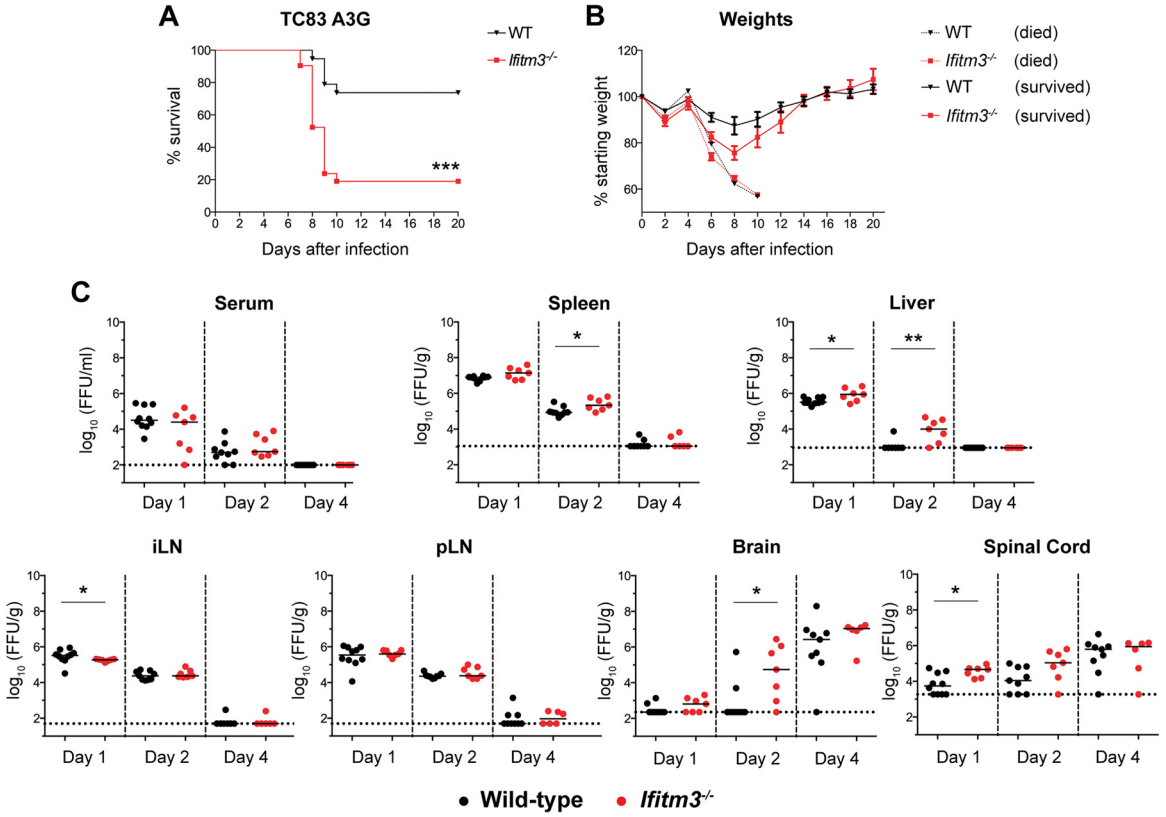

FIG 7 Ifitm3 protects against VEEV pathogenesis. (A and B) Four-week-old WT and *Ifitm3*$^{-/-}$ mice were infected with 10^6 FFU of VEEV-TC83-A3G in the footpad and followed for survival (A) and morbidity by weight loss (B). Data are pooled from two independent experiments ($n = 19$ to 21). Asterisks denote statistical differences by log rank test (***, $P < 0.001$). (C) VEEV viral burden of serum, spleen, liver, inguinal lymph nodes (iLN), popliteal lymph nodes (pLN), brain, and spinal cord at days 1, 2, and 4 after infection of WT and *Ifitm3*$^{-/-}$ mice. Data are pooled from four independent experiments, where each dot represents one mouse ($n = 6$ to 10). Dotted lines represent the limit of detection. Asterisks indicate statistical differences by the Mann-Whitney test (*, $P < 0.05$; **, $P < 0.01$).

type-specific antiviral effect of Ifitm3 in the context of VEEV pathogenesis.

A possible antiviral role of IFITM proteins against alphaviruses has not been extensively analyzed. Studies with pseudotyped virions (alphavirus structural proteins and retroviral RNA) initially suggested that IFITMs had little antiviral activity against CHIKV, SINV, and VEEV (reference 28; M. Farzan, unpublished observations). It remains uncertain why Ifitm3 would not inhibit pseudotyped alphavirus virions although the icosahedral display of E1 and E2 may be altered in these viruses, which could affect entry and fusion of virus particles. Ifitm3 has been implicated, although not definitively demonstrated, as a restriction factor for alphaviruses. Karki et al. identified *IFITM3* as one of 31 human ISGs that functioned synergistically with zinc finger antiviral protein (ZAP) to enhance restriction of SINV infection (50). Schoggins et al. reported that IFITM3 moderately reduced CHIKV and ONNV infection in human cells ectopically expressing IFITM3 (49, 71). Consistent with these observations, a recent paper reported an inhibitory effect of IFITM3 and IFITM1 against SFV and SINV when ectopically expressed in human A549 cells (47). These data support our findings of an antiviral activity of Ifitm3 against multiple alphaviruses.

The characterization of Ifitm3 as an antiviral ISG against alphaviruses adds to the known host defense genes that block alphavirus infection. ISG15 protects against SINV *in vivo*, likely via conjugation (ISGylation) to viral proteins (40–42); ZAP restricts SINV, Ross River virus, SFV, and VEEV by blocking the accumulation of viral genomes in the cytoplasm (72); and BST-2 (tetherin) prevents CHIKV egress by retaining budding virus on the plasma membrane (43). SINV also is strongly inhibited by protein kinase R (PKR) in the context of replication in dendritic cells (DCs) (44). Finally, a separate genetic screen revealed several unique ISGs with possible antiviral activity against SINV, including Isg20, Ifit1, Ifit2, Ifit3, and Rsad2 (viperin) (45).

In studies with other viruses, IFITM3 appears to restrict early steps in the viral life cycle, particularly fusion into the cytoplasm (24–26). This is supported by data from our FFWO experiments in the context of CHIKV infection and by recent studies with SFV (47). However, it remains possible that IFITM3, akin to effects on HIV, could restrict alphavirus infection in a pH-insensitive manner by integrating into the viral membrane, which we are currently exploring using mass spectrometric analysis of alphavirus virions derived from cells expressing or lacking Ifitm3. An additional mechanism that warrants investigation is the possible role for Ifitm3 in preventing viral budding and/or egress. IFITM3 can be detected at the plasma membrane, and its expression and localization are enhanced upon IFN stimulation (18, 65, 66).

In summary, we have shown that Ifitm3 can restrict several alphaviruses both *in vitro* and *in vivo*. Our data in mice suggest

that Ifitm3 may function to restrict early replication and dissemination of alphaviruses, thereby preventing pathogenesis. Further investigation into additional mechanisms of Ifitm3-mediated restriction of alphaviruses is warranted as well as effects of gene polymorphisms, which could contribute to relative disease susceptibility in humans. Indeed, a common human allelic IFITM3 variant, rs12252-C, encodes a 21-amino-acid deletion of the N-terminal part of the protein that appears to be associated with susceptibility to IAV infection (19–21). It remains to be determined whether this or other polymorphisms in the *IFITM3* gene can be linked to more severe or persistent alphavirus infection.

ACKNOWLEDGMENTS

National Institutes of Health grants U19 AI083019, R01 AI104972, and R01 AI089591 supported this study. Research reported in this publication was supported by the National Institute of Arthritis and Musculoskeletal and Skin Diseases, part of the National Institutes of Health, under award number P30AR048335.

Experimental support for the speed congenic backcrossing was provided by the Washington University facility of the Rheumatic Diseases Core Center.

FUNDING INFORMATION

This work, including the efforts of Michael Diamond, was funded by HHS | NIH | National Institute of Allergy and Infectious Diseases (NIAID) (R01 AI104972). This work, including the efforts of Michael Diamond, was funded by HHS | NIH | National Institute of Allergy and Infectious Diseases (NIAID) (U19 AI083019). This work, including the efforts of Michael Diamond, was funded by HHS | NIH | National Institute of Allergy and Infectious Diseases (NIAID) (R01 AI089591).

REFERENCES

1. **Diamond MS, Farzan M.** 2013. The broad-spectrum antiviral functions of IFIT and IFITM proteins. Nat Rev Immunol **13:**46–57. http://dx.doi.org/10.1038/nri3344.
2. **Friedman RL, Manly SP, McMahon M, Kerr IM, Stark GF.** 1984. Transcriptional and posttranscriptional regulation of interferon-induced gene expression in human cells. Cell **38:**745–755.
3. **Siegrist F, Ebeling M, Certa U.** 2011. The small interferon-induced transmembrane genes and proteins. J Interferon Cytokine Res **31:**183–197. http://dx.doi.org/10.1089/jir.2010.0112.
4. **Chesarino NM, McMichael TM, Yount JS.** 2014. Regulation of the trafficking and antiviral activity of IFITM3 by post-translational modifications. Future Microbiol **9:**1151–1163. http://dx.doi.org/10.2217/fmb.14.65.
5. **Smith R, Young J, Weis JJ, Weis JH.** 2006. Expression of the mouse fragilis gene products in immune cells and association with receptor signaling complexes. Genes Immun **7:**113–121. http://dx.doi.org/10.1038/sj.gene.6364278.
6. **Ling S, Zhang C, Wang W, Cai X, Yu L, Wu F, Zhang L, Tian C.** 2016. Combined approaches of EPR and NMR illustrate only one transmembrane helix in the human IFITM3. Sci Rep **6:**24029. http://dx.doi.org/10.1038/srep24029.
7. **Brass AL, Huang I-C, Benita Y, John SP, Krishnan MN, Feeley EM, Ryan BJ, Weyer JL, Van Der Weyden L, Fikrig E, Adams J, Xavier RJ, Farzan M, Elledge SJ.** 2009. The IFITM proteins mediate cellular resistance to influenza A H1N1 virus, West Nile virus, and dengue virus. Cell **139:**1243–1254. http://dx.doi.org/10.1016/j.cell.2009.12.017.
8. **Mudhasani R, Tran JP, Retterer C, Radoshitzky SR, Kota KP, Altamura LA, Smith JM, Packard BZ, Kuhn JH, Costantino J, Garrison AR, Schmaljohn CS, Huang I-C, Farzan M, Bavari S.** 2013. IFITM-2 and IFITM-3 but not IFITM-1 restrict Rift Valley fever virus. J Virol **87:**8451–8464. http://dx.doi.org/10.1128/JVI.03382-12.
9. **Huang I-C, Bailey CC, Weyer JL, Radoshitzky SR, Becker MM, Chiang JJ, Brass AL, Ahmed AA, Chi X, Dong L, Longobardi LE, Boltz D, Kuhn JH, Elledge SJ, Bavari S, Denison MR, Choe H, Farzan M.** 2011. Distinct patterns of IFITM-mediated restriction of filoviruses, SARS coronavirus, and influenza A virus. PLoS Pathog **7:**e1001258. http://dx.doi.org/10.1371/journal.ppat.1001258.
10. **Lu J, Pan Q, Rong L, He W, Liu- SL, Liang C.** 2011. The IFITM proteins inhibit HIV-1 infection. J Virol **85:**2126–2137. http://dx.doi.org/10.1128/JVI.01531-10.
11. **Everitt AR, Clare S, McDonald JU, Kane L, Harcourt K, Ahras M, Lall A, Hale C, Rodgers A, Young DB, Haque A, Billker O, Tregoning JS, Dougan G, Kellam P.** 2013. Defining the range of pathogens susceptible to Ifitm3 restriction using a knockout mouse model. PLoS One **8:**e80723. http://dx.doi.org/10.1371/journal.pone.0080723.
12. **Perreira JM, Chin CR, Feeley EM, Brass AL.** 2013. IFITMs restrict the replication of multiple pathogenic viruses. J Mol Biol **425:**4937–4955. http://dx.doi.org/10.1016/j.jmb.2013.09.024.
13. **Chan YK, Huang I-C, Farzan M.** 2012. IFITM proteins restrict antibody-dependent enhancement of dengue virus infection. PLoS One **7:**e34508. http://dx.doi.org/10.1371/journal.pone.0034508.
14. **Chutiwitoonchai N, Hiyoshi M, Hiyoshi-Yoshidomi Y, Hashimoto M, Tokunaga K, Suzu S.** 2013. Characteristics of IFITM, the newly identified IFN-inducible anti-HIV-1 family proteins. Microbes Infect **15:**280–290. http://dx.doi.org/10.1016/j.micinf.2012.12.003.
15. **Anafu A, Bowen CH, Chin CR, Brass AL, Holm GH.** 2013. Interferon-inducible transmembrane protein 3 (IFITM3) restricts reovirus cell entry. J Biol Chem **288:**17261–17271. http://dx.doi.org/10.1074/jbc.M112.438515.
16. **Jiang D, Weidner JM, Qing M, Pan X-B, Guo H, Xu C, Zhang X, Birk A, Chang J, Shi P-Y, Block TM, Guo J-T.** 2010. Identification of five interferon-induced cellular proteins that inhibit West Nile virus and dengue virus infections. J Virol **84:**8332–8341. http://dx.doi.org/10.1128/JVI.02199-09.
17. **Narayana SK, Helbig KJ, McCartney EM, Eyre NS, Bull RA, Eltahla A, Lloyd AR, Beard MR.** 2015. The interferon-induced transmembrane proteins, IFITM1, IFITM2, and IFITM3 inhibit hepatitis C virus entry. J Biol Chem **290:**25946–25959. http://dx.doi.org/10.1074/jbc.M115.657346.
18. **Bailey CC, Huang I-C, Kam C, Farzan M.** 2012. Ifitm3 limits the severity of acute influenza in mice. PLoS Pathog **8:**e1002909. http://dx.doi.org/10.1371/journal.ppat.1002909.
19. **Everitt AR, Clare S, Pertel T, John SP, Wash RS, Smith SE, Chin CR, Feeley EM, Sims JS, Adams DJ, Wise HM, Kane L, Goulding D, Digard P, Anttila V, Baillie JK, Walsh TS, Hume DA, Palotie A, Xue Y, Colonna V, Tyler-Smith C, Dunning J, Gordon SB, Smyth RL, Openshaw PJ, Dougan G, Brass AL, Kellam P.** 2012. IFITM3 restricts the morbidity and mortality associated with influenza. Nature **484:**519–523. http://dx.doi.org/10.1038/nature10921.
20. **Zhang Y-H, Zhao Y, Li N, Peng Y-C, Giannoulatou E, Jin R-H, Yan H-P, Wu H, Liu J-H, Liu N, Wang D-Y, Shu Y-L, Ho L-P, Kellam P, McMichael A, Dong T.** 2013. Interferon-induced transmembrane protein-3 genetic variant rs12252-C is associated with severe influenza in Chinese individuals. Nat Commun **4:**1418. http://dx.doi.org/10.1038/ncomms2433.
21. **Wang Z, Zhang A, Wan Y, Liu X, Qiu C, Xi X, Ren Y, Wang J, Dong Y, Bao M, Li L, Zhou M, Yuan S, Sun J, Zhu Z, Chen L, Li Q, Zhang Z, Zhang X, Lu S, Doherty PC, Kedzierska K, Xu J.** 2014. Early hypercytokinemia is associated with interferon-induced transmembrane protein-3 dysfunction and predictive of fatal H7N9 infection. Proc Natl Acad Sci U S A **111:**769–774. http://dx.doi.org/10.1073/pnas.1321748111.
22. **Williams DEJ, Wu W-L, Grotefend CR, Radic V, Chung C, Chung Y-H, Farzan M, Huang I-C.** 2014. IFITM3 polymorphism rs12252-C restricts influenza A viruses. PLoS One **9:**e110096. http://dx.doi.org/10.1371/journal.pone.0110096.
23. **Weidner JM, Jiang D, Pan X-B, Chang J, Block TM, Guo J-T.** 2010. Interferon-induced cell membrane proteins, IFITM3 and tetherin, inhibit vesicular stomatitis virus infection via distinct mechanisms. J Virol **84:**12646–12657. http://dx.doi.org/10.1128/JVI.01328-10.
24. **Desai TM, Marin M, Chin CR, Savidis G, Brass AL, Melikyan GB.** 2014. IFITM3 restricts influenza A virus entry by blocking the formation of fusion pores following virus-endosome hemifusion. PLoS Pathog **10:**e1004048. http://dx.doi.org/10.1371/journal.ppat.1004048.
25. **Feeley EM, Sims JS, John SP, Chin CR, Pertel T, Chen L-M, Gaiha GD, Ryan BJ, Donis RO, Elledge SJ, Brass AL.** 2011. IFITM3 inhibits influenza A virus infection by preventing cytosolic entry. PLoS Pathog **7:**e1002337. http://dx.doi.org/10.1371/journal.ppat.1002337.
26. **Li K, Markosyan RM, Zheng Y-M, Golfetto O, Bungart B, Li M, Ding**

S, He Y, Liang C, Lee JC, Gratton E, Cohen FS, Liu S-L. 2013. IFITM proteins restrict viral membrane hemifusion. PLoS Pathog **9:**e1003124. http://dx.doi.org/10.1371/journal.ppat.1003124.

27. **Compton AA, Bruel T, Porrot F, Mallet A, Sachse M, Euvrard M, Liang C, Casartelli N, Schwartz O.** 2014. IFITM proteins incorporated into HIV-1 virions impair viral fusion and spread. Cell Host Microbe **16:**736–747. http://dx.doi.org/10.1016/j.chom.2014.11.001.
28. **Bailey CC, Zhong G, Huang I-C, Farzan M.** 2014. IFITM-family proteins: the cell's first line of antiviral defense. Annu Rev Virol **1:**261–283. http://dx.doi.org/10.1146/annurev-virology-031413-085537.
29. **Lin T-Y, Chin CR, Everitt AR, Clare S, Perreira JM, Savidis G, Aker AM, John SP, Sarlah D, Carreira EM, Elledge SJ, Kellam P, Brass AL.** 2013. Amphotericin B increases influenza A virus infection by preventing IFITM3-mediated restriction. Cell Rep **5:**895–908. http://dx.doi.org/10.1016/j.celrep.2013.10.033.
30. **Lescar J, Roussel A, Wien MW, Navaza J, Fuller SD, Wengler G, Wengler G, Rey FA.** 2001. The fusion glycoprotein shell of Semliki Forest virus: an icosahedral assembly primed for fusogenic activation at endosomal pH. Cell **105:**137–148. http://dx.doi.org/10.1016/S0092-8674(01)00303-8.
31. **Smith TJ, Cheng RH, Olson NH, Peterson P, Chase E, Kuhn RJ, Baker TS.** 1995. Putative receptor binding sites on alphaviruses as visualized by cryoelectron microscopy. Proc Natl Acad Sci U S A **92:**10648–10652. http://dx.doi.org/10.1073/pnas.92.23.10648.
32. **Cheng RH, Kuhn RJ, Olson NH, Rossmann MG, Choi HK, Smith TJ, Baker TS.** 1995. Nucleocapsid and glycoprotein organization in an enveloped virus. Cell **80:**621–630. http://dx.doi.org/10.1016/0092-8674(95)90516-2.
33. **Petersen LR, Powers AM.** 2016. Chikungunya: epidemiology. F1000Res **5:**82. http://dx.doi.org/10.12688/f1000research.7171.1.
34. **Steele KE, Twenhafel N.** 2010. Review paper: pathology of animal models of alphavirus encephalitis. Vet Pathol **47:**790–805. http://dx.doi.org/10.1177/0300985810372508.
35. **Caglioti C, Lalle E, Castilletti C, Carletti F, Capobianchi MR, Bordi L.** 2013. Chikungunya virus infection: an overview. New Microbiol **36:**211–227.
36. **Morrison TE, Oko L, Montgomery SA, Whitmore AC, Lotstein AR, Gunn BM, Elmore SA, Heise MT.** 2011. A mouse model of chikungunya virus-induced musculoskeletal inflammatory disease: evidence of arthritis, tenosynovitis, myositis, and persistence. Am J Pathol **178:**32–40. http://dx.doi.org/10.1016/j.ajpath.2010.11.018.
37. **Couderc T, Chrétien F, Schilte C, Disson O, Brigitte M, Guivel-Benhassine F, Touret Y, Barau G, Cayet N, Schuffenecker I, Desprès P, Arenzana-Seisdedos F, Michault A, Albert ML, Lecuit M.** 2008. A mouse model for Chikungunya: young age and inefficient type-I interferon signaling are risk factors for severe disease. PLoS Pathog **4:**e29. http://dx.doi.org/10.1371/journal.ppat.0040029.
38. **Chen W, Foo S-S, Rulli NE, Taylor A, Sheng K-C, Herrero LJ, Herring BL, Lidbury B, Li RW, Walsh NC, Sims N, Smith PN, Mahalingam S.** 2014. Arthritogenic alphaviral infection perturbs osteoblast function and triggers pathologic bone loss. Proc Natl Acad Sci U S A **111:**6040–6045. http://dx.doi.org/10.1073/pnas.1318859111.
39. **Chen W, Foo SS, Sims NA, Herrero LJ, Walsh NC, Mahalingam S.** 2015. Arthritogenic alphaviruses: new insights into arthritis and bone pathology. Trends Microbiol **23:**35–43. http://dx.doi.org/10.1016/j.tim.2014.09.005.
40. **Lenschow DJ, Giannakopoulos NV, Gunn LJ, Johnston C, O'Guin AK, Schmidt RE, Levine B, Virgin HW.** 2005. Identification of interferon-stimulated gene 15 as an antiviral molecule during Sindbis virus infection in vivo. J Virol **79:**13974–13983. http://dx.doi.org/10.1128/JVI.79.22.13974-13983.2005.
41. **Lenschow DJ, Lai C, Frias-Staheli N, Giannakopoulos NV, Lutz A, Wolff T, Osiak A, Levine B, Schmidt RE, García-Sastre A, Leib DA, Pekosz A, Knobeloch K, Horak I, Virgin HW.** 2007. IFN-stimulated gene 15 functions as a critical antiviral molecule against influenza, herpes, and Sindbis viruses. Proc Natl Acad Sci U S A **104:**1371–1376. http://dx.doi.org/10.1073/pnas.0607038104.
42. **Werneke SW, Schilte C, Rohatgi A, Monte KJ, Michault A, Arenzana-Seisdedos F, Vanlandingham DL, Higgs S, Fontanet A, Albert ML, Lenschow DJ.** 2011. ISG15 is critical in the control of Chikungunya virus infection independent of UbE1L mediated conjugation. PLoS Pathog **7:**e1002322. http://dx.doi.org/10.1371/journal.ppat.1002322.
43. **Jones PH, Maric M, Madison MN, Maury W, Roller RJ, Okeoma CM.** 2013. BST-2/tetherin-mediated restriction of chikungunya (CHIKV) VLP budding is counteracted by CHIKV non-structural protein 1 (nsP1). Virology **438:**37–49. http://dx.doi.org/10.1016/j.virol.2013.01.010.
44. **Ryman KD, Meier KC, Nangle EM, Ragsdale SL, Korneeva NL, Rhoads RE, Macdonald MR, Klimstra WB.** 2005. Sindbis virus translation is inhibited by a PKR/RNase L-independent effector induced by alpha/beta interferon priming of dendritic cells. J Virol **79:**1487–1499. http://dx.doi.org/10.1128/JVI.79.3.1487-1499.2005.
45. **Zhang Y, Burke CW, Ryman KD, Klimstra WB.** 2007. Identification and characterization of interferon-induced proteins that inhibit alphavirus replication. J Virol **81:**11246–11255. http://dx.doi.org/10.1128/JVI.01282-07.
46. **Hyde JL, Gardner CL, Kimura T, White JP, Liu G, Trobaugh DW, Huang C, Tonelli M, Paessler S, Takeda K, Klimstra WB, Amarasinghe GK, Diamond MS.** 2014. A viral RNA structural element alters host recognition of nonself RNA. Science **343:**783–787. http://dx.doi.org/10.1126/science.1248465.
47. **Weston S, Czieso S, White IJ, Smith SE, Wash RS, Diaz-Soria C, Kellam P, Marsh M.** 24 May 2016. Alphavirus restriction by IFITM proteins. Traffic http://dx.doi.org/10.1111/tra.12416.
48. **Schoggins JW, Rice CM.** 2011. Interferon-stimulated genes and their antiviral effector functions. Curr Opin Virol **1:**519–525. http://dx.doi.org/10.1016/j.coviro.2011.10.008.
49. **Schoggins JW, Wilson SJ, Panis M, Murphy MY, Jones CT, Bieniasz P, Rice CM.** 2011. A diverse range of gene products are effectors of the type I interferon antiviral response. Nature **472:**481–485. http://dx.doi.org/10.1038/nature09907.
50. **Karki S, Li MM, Schoggins JW, Tian S, Rice CM, Macdonald MR.** 2012. Multiple interferon stimulated genes synergize with the zinc finger antiviral protein to mediate anti-alphavirus activity. PLoS One **7:**e37398. http://dx.doi.org/10.1371/journal.pone.0037398.
51. **National Research Council.** 2011. Guide for the care and use of laboratory animals, 8th ed. National Academies Press, Washington, DC.
52. **Lange UC, Adams DJ, Lee C, Barton S, Schneider R, Bradley A, Surani MA.** 2008. Normal germ line establishment in mice carrying a deletion of the Ifitm/Fragilis gene family cluster. Mol Cell Biol **28:**4688–4696. http://dx.doi.org/10.1128/MCB.00272-08.
53. **Wakeland E, Morel L, Achey K, Yui M, Longmate J.** 1997. Speed congenics: a classic technique in the fast lane (relatively speaking). Immunol Today **18:**472–477. http://dx.doi.org/10.1016/S0167-5699(97)01126-2.
54. **Pal P, Dowd KA, Brien JD, Edeling MA, Gorlatov S, Johnson S, Lee I, Akahata W, Nabel GJ, Richter MKS, Smit JM, Fremont DH, Pierson TC, Heise MT, Diamond MS.** 2013. Development of a highly protective combination monoclonal antibody therapy against Chikungunya virus. PLoS Pathog **9:**e1003312. http://dx.doi.org/10.1371/journal.ppat.1003312.
55. **Oliphant T, Engle M, Nybakken GE, Doane C, Johnson S, Huang L, Gorlatov S, Mehlhop E, Marri A, Chung KM, Ebel GD, Kramer LD, Fremont DH, Diamond MS.** 2005. Development of a humanized monoclonal antibody with therapeutic potential against West Nile virus. Nat Med **11:**522–530. http://dx.doi.org/10.1038/nm1240.
56. **Oliphant T, Nybakken GE, Engle M, Xu Q, Nelson CA, Sukupolvi-Petty S, Marri A, Lachmi B-E, Olshevsky U, Fremont DH, Pierson TC, Diamond MS.** 2006. Antibody recognition and neutralization determinants on domains I and II of West Nile virus envelope protein. J Virol **80:**12149–12159. http://dx.doi.org/10.1128/JVI.01732-06.
57. **Lazear HM, Pinto AK, Vogt MR, Gale M, Diamond MS.** 2011. Beta interferon controls West Nile virus infection and pathogenesis in mice. J Virol **85:**7186–7194. http://dx.doi.org/10.1128/JVI.00396-11.
58. **Dora S, Schwarz C, Baack M, Graessmann A, Knippers R.** 1989. Analysis of a large-T-antigen variant expressed in simian virus 40-transformed mouse cell line mKS-A. J Virol **63:**2820–2828.
59. **Araki T, Sasaki Y, Milbrandt J.** 2004. Increased nuclear NAD biosynthesis and SIRT1 activation prevent axonal degeneration. Science **305:**1010–1013. http://dx.doi.org/10.1126/science.1098014.
60. **Cho H, Proll SC, Szretter KJ, Katze MG, Gale M, Diamond MS.** 2013. Differential innate immune response programs in neuronal subtypes determine susceptibility to infection in the brain by positive-stranded RNA viruses. Nat Med **19:**1–8. http://dx.doi.org/10.1038/nm.3061.
61. **Tsetsarkin K, Higgs S, McGee CE, De Lamballerie X, Charrel RN, Vanlandingham DL.** 2006. Infectious clones of Chikungunya virus (La Réunion isolate) for vector competence studies. Vector Borne Zoonotic Dis **6:**325–337. http://dx.doi.org/10.1089/vbz.2006.6.325.
62. **Morrison TE, Whitmore AC, Shabman RS, Lidbury BA, Mahalingam S, Heise MT.** 2006. Characterization of Ross River virus tropism and virus-

induced inflammation in a mouse model of viral arthritis and myositis. J Virol **80:**737–749. http://dx.doi.org/10.1128/JVI.80.2.737-749.2006.

63. **Smith SA, Silva LA, Fox JM, Flyak AI, Kose N, Sapparapu G, Khomandiak S, Ashbrook AW, Kahle KM, Fong RH, Swayne S, Doranz BJ, McGee CE, Heise MT, Pal P, Brien JD, Austin SK, Diamond MS, Dermody TS, Crowe JE.** 2015. Isolation and characterization of broad and ultrapotent human monoclonal antibodies with therapeutic activity against chikungunya virus. Cell Host Microbe **18:**86–95. http://dx.doi.org/10.1016/j.chom.2015.06.009.
64. **Wahlberg JM, Garoff H.** 1992. Membrane fusion process of Semliki Forest virus. I: Low pH-induced rearrangement in spike protein quaternary structure precedes virus penetration into cells. J Cell Biol **116:**339–348.
65. **Bailey CC, Kondur HR, Huang I-C, Farzan M.** 2013. Interferon-induced transmembrane protein 3 is a type II transmembrane protein. J Biol Chem **288:**32184–32193. http://dx.doi.org/10.1074/jbc.M113.514356.
66. **Amini-Bavil-Olyaee S, Choi YJ, Lee JH, Shi M, Huang I-C, Farzan M, Jung JU.** 2013. The antiviral effector IFITM3 disrupts intracellular cholesterol homeostasis to block viral entry. Cell Host Microbe **13:**452–464. http://dx.doi.org/10.1016/j.chom.2013.03.006.
67. **Edwards J, Brown DT.** 1986. Sindbis virus-mediated cell fusion from without is a two-step event. J Gen Virol **67:**377–380. http://dx.doi.org/10.1099/0022-1317-67-2-377.
68. **Hawman DW, Stoermer K, Montgomery S, Pal P, Oko L, Diamond MS, Morrison TE.** 2013. Chronic joint disease caused by persistent Chikungunya virus infection is controlled by the adaptive immune response. J Virol **87:**13878–13888. http://dx.doi.org/10.1128/JVI.02666-13.
69. **Fros JJ, Major LD, Scholte FEM, Gardner J, Van Hemert MJ, Suhrbier A, Pijlman GP.** 2015. Chikungunya virus non-structural protein 2-mediated host shut-off disables the unfolded protein response. J Gen Virol **96:**580–589. http://dx.doi.org/10.1099/vir.0.071845-0.
70. **Hollidge BS, Weiss SR, Soldan SS.** 2011. The role of interferon antagonist, non-structural proteins in the pathogenesis and emergence of arboviruses. Viruses **3:**629–658. http://dx.doi.org/10.3390/v3060629.
71. **Schoggins JW, MacDuff DA, Imanaka N, Gainey MD, Shrestha B, Eitson JL, Mar KB, Richardson RB, Ratushny AV, Litvak V, Dabelic R, Manicassamy B, Aitchison JD, Aderem A, Elliott RM, García-Sastre A, Racaniello V, Snijder EJ, Yokoyama WM, Diamond MS, Virgin HW, Rice CM.** 2014. Pan-viral specificity of IFN-induced genes reveals new roles for cGAS in innate immunity. Nature **505:**691–695. http://dx.doi.org/10.1038/nature12862.
72. **Bick MJ, Carroll JN, Gao G, Goff SP, Rice CM, MacDonald MR.** 2003. Expression of the zinc-finger antiviral protein inhibits alphavirus replication. J Virol **77:**11555–11562. http://dx.doi.org/10.1128/JVI.77.21.11555-11562.2003.
73. **Gorman MJ, Poddar S, Farzan M, Diamond MS.** 2016. The interferon-stimulated gene IFITM3 restricts West Nile virus infection and pathogenesis. J Virol **90:**8212–8225. http://dx.doi.org/10.1128/JVI.00581-16.